Georgia State University

ScholarWorks @ Georgia State University

Chemistry Theses   Department of Chemistry

12-2009

The Kinetics of Epoxidation of A,B-Unsaturated Esters by Dimethyldioxirane: A Mechanistic Study

John P. Sansone

Georgia State University, jsansone1@student.gsu.edu

Follow this and additional works at: https://scholarworks.gsu.edu/chemistry_theses

THE KINETICS OF EPOXIDATION OF A,B-UNSATURATED ESTERS BY

DIMETHYLDIOXIRANE: A MECHANISTIC STUDY

by

JOHN P. SANSONE

Under the Direction of Alfons Baumstark

ABSTRACT

The epoxidation of a series of α,β-unsaturated esters by dimethyldioxirane was studied. Second

order rate constants were determined under pseudo first order conditions. The epoxide of each

ester upon full conversion was found to be the only isolable product. Second order rate constants

for the cis-like ethyl tiglate showed a 4 fold increase over that of trans-like angelic methyl ester.

The ester substituent was found to have little effect on overall rate constants. A comparison of a

relatively strained cyclopentene carboxylate to the cyclohexene carboxylate showed a 2 fold

increase in selectivity for the former. Ethyl methacrylate displayed unexpected reactivity toward

dioxirane; undergoing reaction faster than more substituted electron rich alkenes. Computer

modeling studies using the AM-1 and density functional approaches were carried out to gain

insights into the mechanistic aspects of the reaction. The esters in general favored the S-cis

conformation or were evenly distributed among S-cis and S-trans except for the ethyl

methacrylate case. The AM-1 approach did not predict the reactivity of open chain esters. The density functional approach predicted the relative reactivity of seven of the nine esters but could not predict the reactivity when the R1 group was substituted. One possible explanation is that the computer model predicts the methyl groups of the dioxirane to be positioned over the R1 group in the lowest energy of all other esters, but steric clash prevents this for angelic methyl ester and ethyl 3,3 dimethyl acrylate.

INDEX WORDS: Kinetics, Dimethyldioxirane, Epoxidation, Computer modeling

THE KINETICS OF EPOXIDATION OF A,B-UNSATURATED ESTERS BY

DIMETHYLDIOXIRANE: A MECHANISTIC STUDY

by

JOHN P. SANSONE

A Thesis Submitted in Partial Fulfillment of the Requirements for the Degree of

Master of Science

in the College of Arts and Sciences

Georgia State University

2009

THE KINETICS OF EPOXIDATION OF A,B-UNSATURATED ESTERS BY

DIMETHYLDIOXIRANE: A MECHANISTIC STUDY

by

JOHN P. SANSONE

	Committee Chair:	Alfons Baumstark
	Committee:	Pedro Vasquez
		Markus Germann

Electronic Version Approved: Aug 2009

Office of Graduate Studies
College of Arts and Sciences
Georgia State University
December 2009

TABLE OF CONTENTS

LIST OF TABLES

LIST OF FIGURES

Introduction
A. History

Dioxiranes are selective and potent oxygen transfer reagents. Historically, The three membered cyclic peroxides are used in difficult oxygen transfer reactions such as oxygen insertion into tertiary C-H bonds[1], or in some cases to create an enantiomeric excess during a synthetic epoxidation reaction[2].

The existence of a dioxirane was proposed as early as 1899 as an intermediate in the famous Baeyer-Villager oxidation[3], although it is now thought that there are in fact no dioxirane intermediates involved in this reaction (Reaction 1).
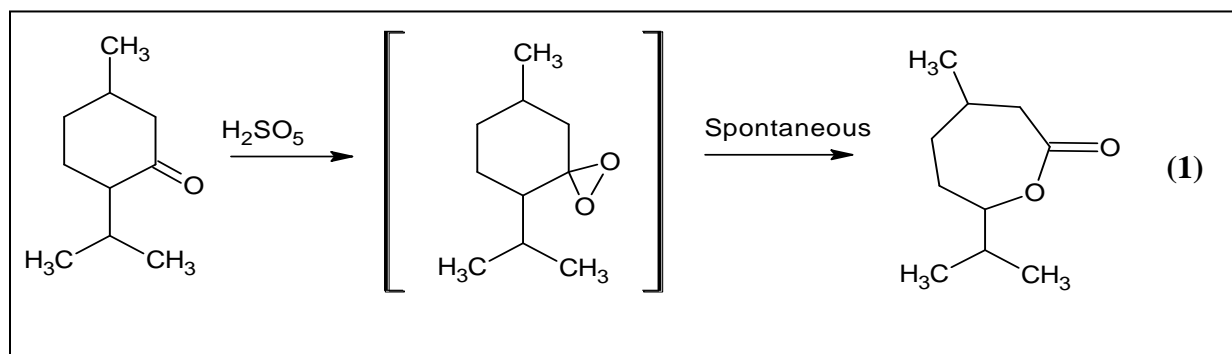
In 1972 the first dioxirane synthesis patent was filled for the synthesis of trifluorodimethyldioxirane by Talbott and Thompson[4]. The synthesis involved the reaction of the dilithium alkoxy precursor with F_2 under Argon atmosphere (Reaction 2).
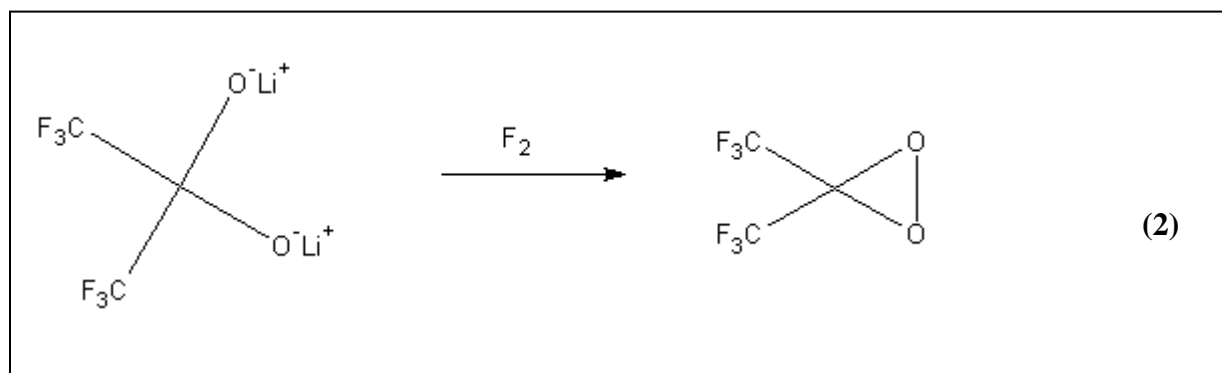
The synthesis yielded a pale yellow solution which could then be purified by low temperature gas chromatography. The resulting perfluorodioxirane solution was then analyzed by ^{19}FNMR, and Mass spectrometry. Further physical evidence of dioxiranes came five years later when Martinez et. al. detected The parent compound via low temperature gas chromatography using a mass spectrum detector[5] in 1977. One year later Suenram and Lovas characterized the bond lengths and dipole moment of unsubtituted dioxirane created during the reaction of ozone with ethylene using microwave spectrometry[6] (Figure 1).
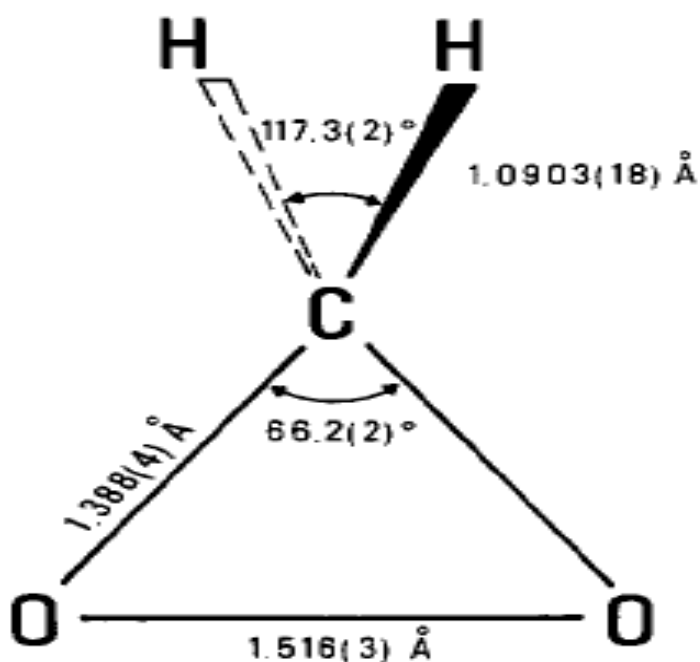
Figure 1: The geometry of dioxirane as determined by microwave spectroscopy[6].

Enriched [18]O studies were used by Curci and coworkers to provide evidence of dioxirane intermediates in the caroate/ketone system[7]. The researchers showed that not only was the caroate system a powerful oxygen transfer system, but that it also displayed stereoselectivity,

yielding in many cases only one stereoisomer of the product. Curci proposed a mechanism of dimethyldioxirane formation in the caroate system based on the study (Reaction 3).

(3)
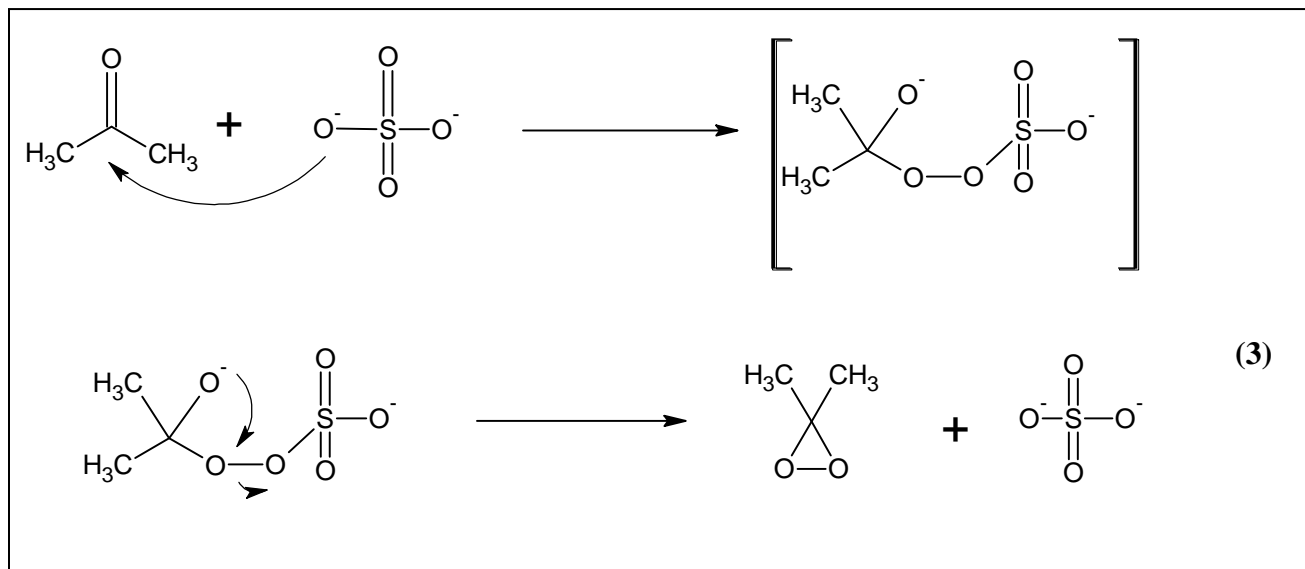
In 1989 Murray developed a procedure to isolate dimethyldioxirane from the caroate/acetone system[8]. Dimethyldioxirane was isolated by vacuum distillation and collected in a vessel at low temperature. Further low pressure distillation of the dioxirane yields a pale yellow solution of between 0.08 and 0.11 molar dioxirane in acetone. The isolation of dimethyldioxirane allowed physical data of the compound to be collected. Most importantly for kinetic research, UV spectroscopy experiments of dioxirane in acetone yielded a λ_{Max} of 335 nm with a molar absorptivity of $\varepsilon = 12.9$ cm^{-1} M^{-1}. Infrared spectroscopy experiments have shown major absorptions for dimethyldioxirane at 1209 cm^{-1}, 1094 cm^{-1}, and 899cm^{-1}. A proton NMR spectrum of dimethyldioxirane shows only one absorption at 1.65ppm.

B. Reactions of Dimethyldioxirane

Dimethyldioxirane has been shown to be a very versatile oxygen transfer reagent as both a distilled solution (in acetone) and *in situ* as part of the acetone/caroate system. In general terms dimethyldioxirane is known to epoxidize a number of alkenes (Reaction 4) from simple alkenes, to sterically hindered alkenes, to electron poor α,β-unsaturated alkenes[9,10,].

(4)
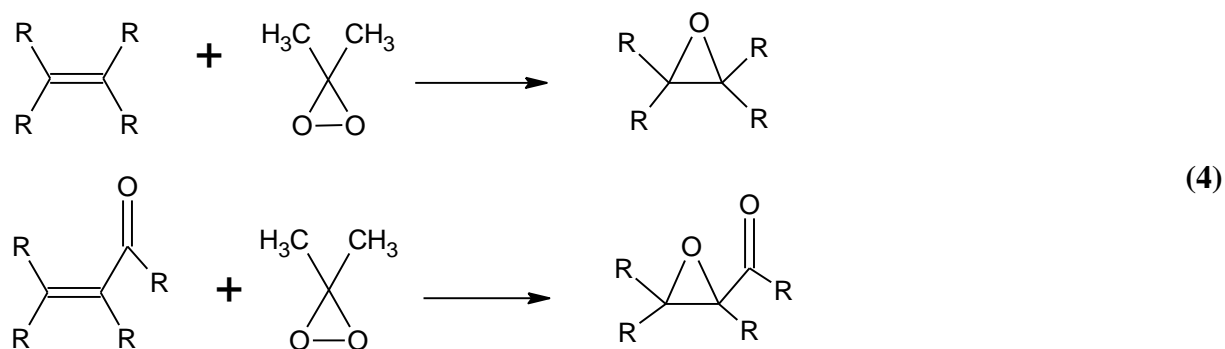
Dioxirane has also been used to oxidize sulfide bonds to sulfoxides and on to sulfones (Reaction 5) when reacted with excess dioxirane[11].

(5)
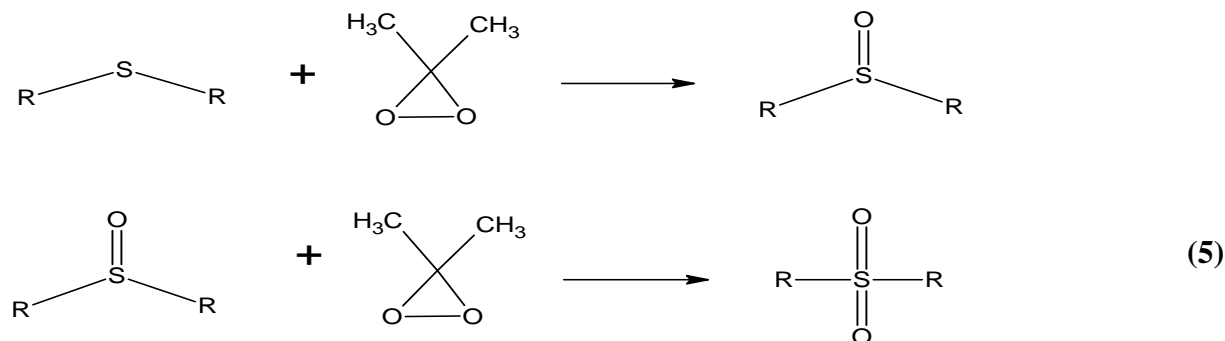
Secondary aliphatic and aromatic amines can undergo an oxygen insertion to form a new N-O bond (Reaction 6), while primary amines can form the corresponding nitro compound[14].

R= aliphatic, or aromatic

(6)
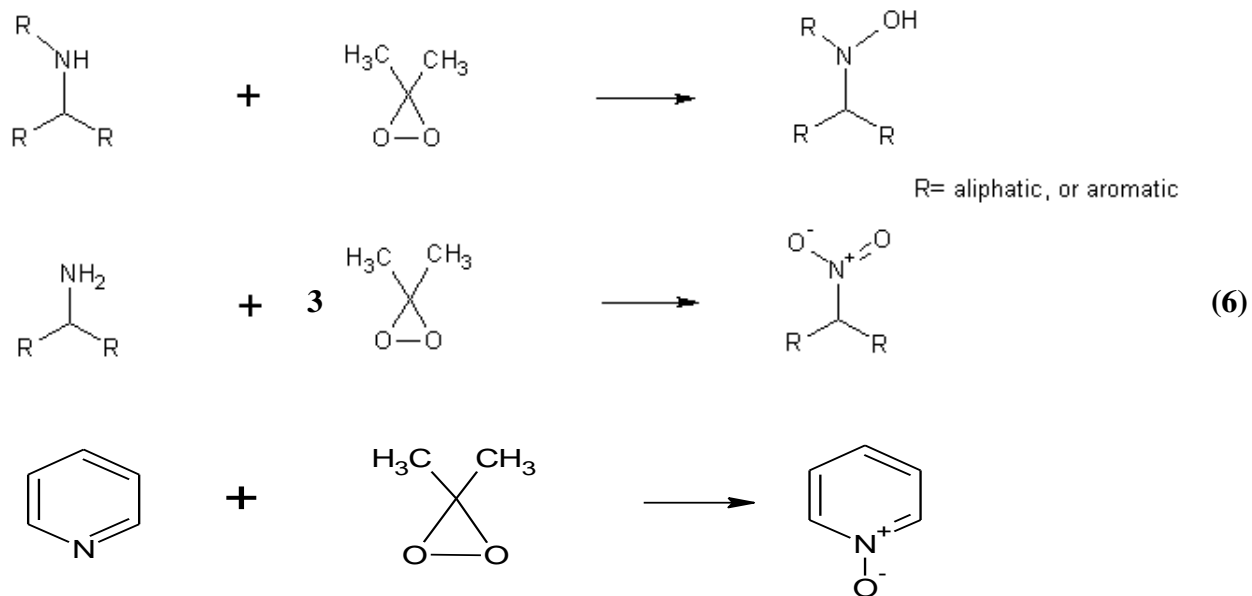
Dimethyl dioxirane will also oxidize secondary alcohols to ketones (Reaction 7), as well as aldehydes to carboxylic acids[12,13].

(7)
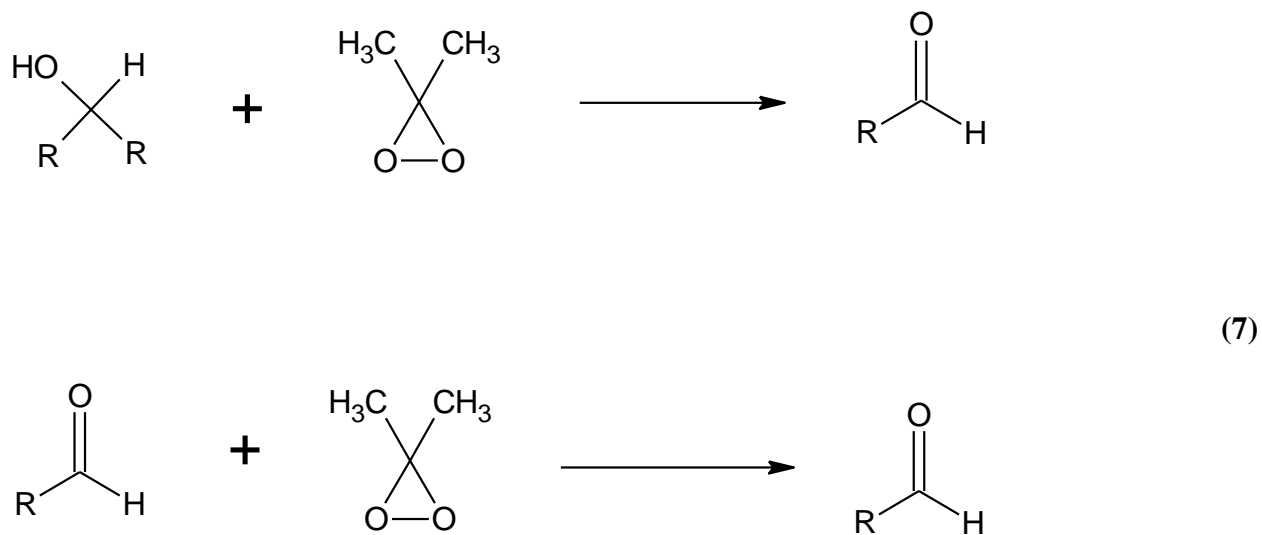
The reaction of dimethyldioxirane with a series of ethers has been shown to produce the

corresponding alcohol and ketone presumably via the corresponding α-hydroxy ethers[15] which

spontaneously decomposes (Reaction 8).

(8)
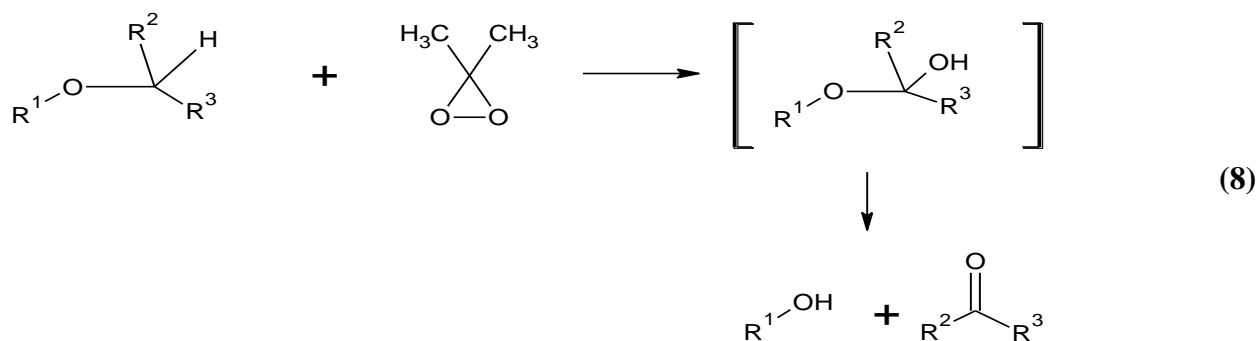
One relatively unique reaction of dimethyldioxirane is ability to insert an oxygen atom in to a

tertiary carbon center at room temperature under mild conditions. The final result is to convert an

otherwise unreactive C-H sigma bond into a new C-OH bond[16] (Reaction 9).

(9)
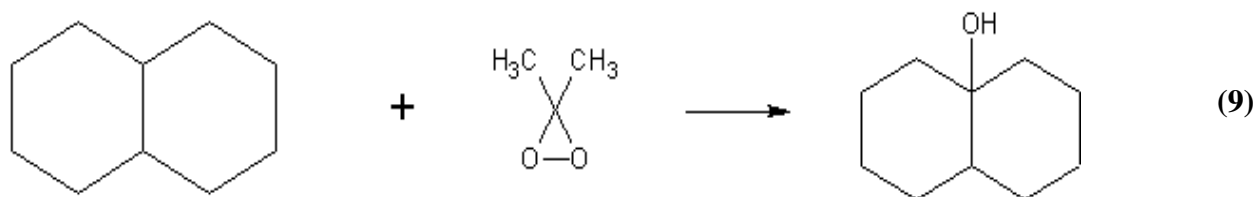
The general reactions above along with numerous others have drastically increased interest in

dioxirane chemistry. For example, the ability to insert an oxygen atom into a carbon sigma bond

has peaked interest in dioxiranes as a method to functionalized the so-called nanodiamonds

adamante and diamante[17]. Outside of the research community, chemistry industry has recently looked into employing dioxirane in bleaching reactions for products like wood pulps[18].

C. Relative Reactivity

The relative reactivity of many of the above reactions has been determined. Kinetic experiments carried out under equal conditions has been used to compare the relative reactivity many of the reactions of dioxirane. The conditions of every reaction are kept constant by using a water bath to control temperature, maintaining dried conditions, and minimizing the presence of metal ions by cleaning all glassware with a chelating agent. The k_2 value of a reaction can then be found under these specific conditions and compared to determine the relative reactivity of certain compounds with dimethyldioxirane.

Of the reactions listed above hetero atoms have been found to be the most reactive toward dioxirane. The hetero oxidation of phosphorus would take place faster than that of sulfer in the same conditions. Amines are the least reactive toward dioxirane in this group of reactions (Table 1).

Table 1: Typical k_2 ranges for a series of selected sulfides, sulfoxides, and nitrogen containing aromatics with dimethyldioxirane at room temperature.

Class	k_2 range ($M^{-1} s^{-1}$)
Aryl methyl sulfide[11]	$3.7 \times 10^1 - 3.8 \times 10^2$
Aryl methyl sulfoxide[11]	$4.6 \times 10^1 - 8 \times 10^2$
Pyridines[14]	$7 \times 10^{-1} - 1.4 \times 10^{-2}$
Quinoline[14]	$3.3 \times 10^{-1} - 1.1 \times 10^{-1}$
Isoquinoline[14]	$1.47 - 1.01$

Alkenes are generally less reactive toward dimethyldioxirane than hetero atoms. Kinetic experiments have elucidated a dramatic difference in reactivity among alkenes based on both steric and electronic effects. For example cis 2-butene was found to undergo reaction about seven times faster than trans 2-butene[19], with other cis/trans pairs following a similar pattern. Electronically it was found that electron releasing alkyl groups will increase the observed k value by about an order of magnitude per added substitution level (ie. primary < secondary < tertiary). Consequently the addition of an electron withdrawing carbonyl group conjugated to the alkene moiety will decrease the kinetic value on the order of 2000 times[20]. Table 2 summarizes ranges of k_2 values found for reactions of diethyldioxirane with alkenes.

Table 2: Typical k_2 ranges for a series of selected alkenes with dimethyldioxirane at room temperature.

Class	k_2 range ($M^{-1}\,s^{-1}$)
Simple cis alkenes[19]	4.6×10^{-1} - 4.7×10^{-2}
Simple trans alkenes[21]	8.4×10^{-2} - 1.2×10^{-2}
Alkyl dienes[20]	8.7×10^{-1} - 3.83
α,β-unsaturated ketones[20]	6.2×10^{-2} - 2.1×10^{-4}
α,β-unsaturated esters[20]	2.4×10^{-2} - 1.7×10^{-4}

Secondary alcohols and ethers are generally less reactive toward oxygen insertion by dimethyldioxirane than alkenes are toward epoxidation. Among secondary alcohols open chain alcohols are slightly more reactive than cyclic secondary alcohols. The oxidation of secondary

alcohols occurs at least 10 times faster than the corresponding methyl ether. Table 3 summarizes expected k_2 values of secondary alcohols and ethers.

Table 3: Typical k_2 ranges for a series of selected secondary alcohols and ethers with dimethyldioxirane at room temperature.

Class	k2 range (M^{-1} s^{-1})
Secondary OH [12,22]	2.24×10^{-2} - 3.8×10^{-3}
Cyclic secondary OH	6.4×10^{-2} - 5.4×10^{-3}
Dialkyl ethers [15]	6.8×10^{-4} – 3×10^{-4}
Alkyl benzyl ethers [23]	1.85×10^{-2} – 9.45×10^{-3}

The ranges given above are typical examples of what should be expected for a certain family of compounds. It should be noted that most families can display rather large ranges of reactivity due to the high sensitivity of dioxirane to electronic and steric effects. There is much overlap between each family because of the large ranges.

D. Mechanistic studies

Most mechanistic studies of dimethyldioxirane chemistry fall in to two categories. The first studies experimentally examined the nature of the attack i.e does the dioxirane undergo a nucleophilic attack, an electrophilic attack, proceed through a radical mechanism, or have a so called biphilic nature. Later computer modeling studies were incorporated to explore the

transition state geometry, as well as further explore a possible radical or carbonyl oxide intermediate in the reaction.

Experiments involving Hammet constants have been used extensively to study the nucleophilic/electrophilic nature of dimethyl dioxirane with uniform results. For example Murray and Shiang explored the Hammet constant of the highly electron poor alkene moiety of ethyl cinnimate[24] finding a value of $\sigma = -1.53$, which is indicative of an electophilic oxygen transfer. Hanson et. al. found similar results in a study of the kinetics of aryl methyl sulfides[11], with hammet σ values in the range of -0.54 to -1.13 in a variety of solvents. Several such experiments exist, all seemingly supporting an electrophilic mechanism of dimethyldioxirane.

In 2001 Duebel challenged the idea that the epoxidation of alkenes always proceeds with a nucleophilic attack of the alkene on the dioxirane with computational models that suggested a biphilic character[25]. The idea of a biphilic dimethyldioxirane which acts as a nucleophile on electron poor alkenes and an electrophile when the alkene is electron rich was refuted by Curci and co-workers[26] in 2007. Experimentally Curci sighted a previous study of the very electron poor ethyl cinnimate family. The experimentally determined σ value for dimethyldioxirane with the family was found to be -0.91 further supporting the electrophilic hypothesis. Furthermore, computer modeling at the density functional level by Duebel failed to support a biphilic character in any case.

The mechanism of the reaction of the oxygen insertion reaction of dimethyldioxirane with unfunctionalized C-H bonds has been one of intense debate over the years. Early kinetic evidence of oxyfunctionalization of alkanes yielded a clean second order rate which does not support a radical mechanism[27]. Also the reaction proceeds with stereoselectivity suggesting that the reaction is not initiated by a radical since one would expect to see rearranged products.

Experiments to probe for a possible diradical intermediate have shown little evidence of a radical. A current theory proposed is that a caged diradical may be involved in the transition state during widening of the O-O bond. It was thought that a caged radical should show some leakage leading to chlorinated products by reaction of the radical with dichloromethane or chloroform solvent[28]. Some experimental evidence of a radical pathway was found later by reaction of adamantine[29] with dimethyldioxirane under inert atmosphere, and or addition of CCl_3Br. The reaction follows a composite rate law in the absence of the O_2 radical scavenger that was likely the normal second order reaction mixed with a side reaction following a radical mechanism. Molecular modeling studies at the B3LYP level carried out by Freccero and coworkers confirmed the possibility of radical pair formation in the O-insertion into isobutane[30].

The notional of a carbonyl oxide intermediate was studied by Shaffer and Kim in 2000 by computational methods[31]. Their study found a huge energy barrier of 23.2 kcal/mol for the rearrangement of dioxirane to carbonyl oxide, suggesting that the rearrangement is not likely during the reaction.

The geometry of the transition state epoxidation of alkenes has been extensively studied via kinetic data and computational approaches. Kinetic experiments led researchers to the idea of a concerted S_N2-like mechanism. Computer models were used to calculate the geometry and energy of the transition state and allowing for the calculation of the energy of activation for the epoxidation of simple alkenes. The calculated energy of activation was then used to calculate k_{rel} values for the alkenes which could then be compared to experimental findings. The currently held spiro transition state (Figure 2), as opposed to a planar transition state (figure 3), was first proposed by Baumstark to explain the unusual selectivity of dimethyldioxirane in the epoxidation of cis-2-butene vs. trans-2-butene[32].
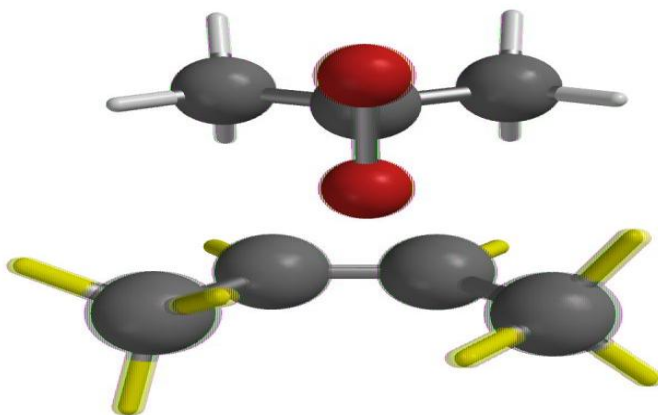
Figure 2: Visualization of the spiro transition[32] state where an imaginary line drawn through the methyl groups of the dimethyldioxirane would run parallel to the carbon-carbon double bond. Hydrogen atoms excluded, bonds to hydrogens shown in white and yellow*
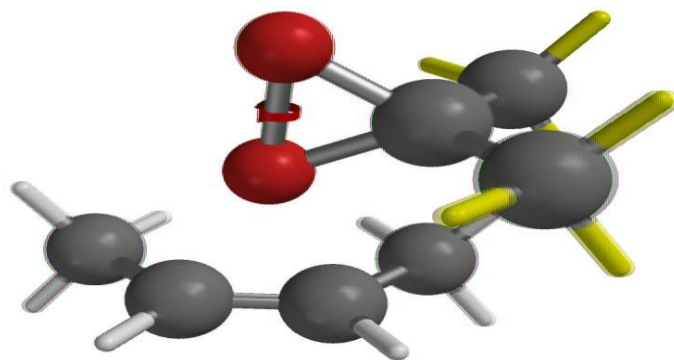
Figure 3: Visualization of the classic butterfly transition state where an imaginary line drawn through the methyl groups of the dimethyldioxirane would run perpendicular to the carbon-carbon double bond.

Hydrogen atoms excluded, bonds to hydrogens shown in white and yellow*

E. Research Statement

Mechanistic studies over the years have undoubtedly helped spark the continually growing interest in dioxirane chemistry as a powerful method for quick, efficient, and selective oxygen transfer processes. The kinetics approach has been used extensively by this group to elucidate the mechanism of oxygen transfer in epoxidations. An understanding of the mechanism may aid the understanding of the origins of the selectivity of dimethyldioxirane, and lead to development of more selective dioxiranes or aid in the use of dimethyldioxirane in synthesis. For example kinetics studies revealed that dimethyldioxirane has a 7 fold higher affinity to undergo reaction with cis-2-butene over trans-2-butene showing the sensitivity of dioxirane to steric influences. A study comparing alkenes of differing levels of substitution showed roughly a ten-fold increase in selectivity for alkenes having a higher level of substitution (i.e trisubstituted alkenes undergo reaction 10 times faster than disubstituted). The increase in selectivity for alkenes having more electron releasing substituents demontrated the sensitivity of dimethyldioxirane to the electron density of the alkene.

In order to build a more complete understanding of dioxirane chemistry a mechanistic study of the reaction of dimethyldioxirane with a series of α,β-unsaturated esters will be carried out. With a large body of kinetic and computer modeling studies carried out already, much is known about the major factors that influence reactivity with dimethyldioxirane. These less reactive, electron poor alkenes should give insight into more subtle factors. For example a major focus of this work is to examine how rotation about the sigma bond between the alkene and carbonyl groups i.e. S-cis/S-trans isomerism will affect the overall rate constants. Ground state equilibrium computer models will be used to predict the relative amount of each conformer present at room temperature. Computer models will aid in examining what factors affect this

equilibrium, and subsequently how will that equilibrium affect the energy of the transition state with dimethyldioxirane. The accuracy of the AM-1 and density functional models will also be compared. For earlier studies the AM-1 model gave results in good agreement with kinetic experiments. More recently however, the AM-1 approach was found to be insufficient to describe α,β-unsaturated ketones. This study will further examine the usefulness of AM-1 calculations for α,β-unsaturated alkenes. Similarly the density functional model will be used to see if it can accurately predict the relative reactivity of α,β-unsaturated esters.

Second order rate constants will be determined to investigate factors that affect reactivity, by investigating selectivity between unsubstituted, mono, and disubstituted α,β-unsaturated esters, the impact of electron donating alkyl groups around the alkene can be examined. Rate constants for ethyl crotonate and tert-butyl crotonate will give insight into the effect of substitution at the alkoxy moiety. Finally, two cyclic ester differing by the size of the ring will be studied to determine how ring size may affect overall reactivity.

A product study will be undertaken to study the outcome of the reaction. Will each ester yield only the corresponding epoxide? NMR spectra of the products will also be used to search for side reactions, or possible rearrangement during the reaction leading to unforeseen products.

Results
A: Product Studies

Product studies of esters **1-9** (Table 4) were carried out. Each ester was allowed to undergo reaction with excess dimethyldioxirane. The resulting reaction mixtures were analyzed by GC/MS confirming the epoxides as the only isolable products in every case (Reaction 10).

Table 4: Structure of esters **1-9**.

Ester	R1	R2	R3	R4
1	H	Me	Me	Et
2	H	H	Me	Me
3	Me	H	Me	Me
4	Me	Me	H	Et
5	H	Me	H	Et
6	H	Me	H	t-Bu
7	H	H	H	Et
8	H	$-CH_2- CH_2-CH_2- CH_2-$		Me
9	H	$-CH_2-CH_2-CH_2-$		Me

Esters **1 - 9**   Epoxides **1a - 9a**   (10)
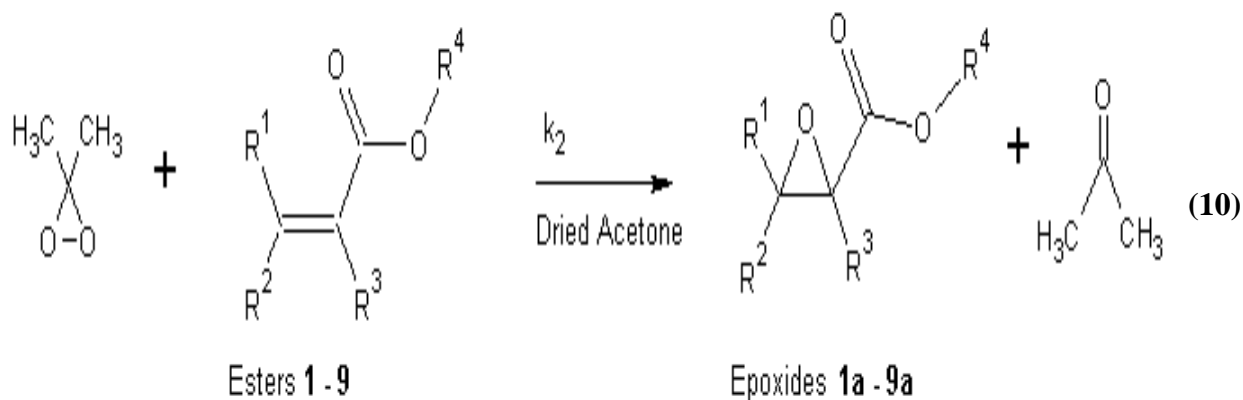
The structure of the distilled products **1a-9a** was further examined by H^1 and C^{13}NMR studies.

Figure 4: ^{1}HNMR spectrum of ethyl tiglate **(1)** in CDCl$_3$.
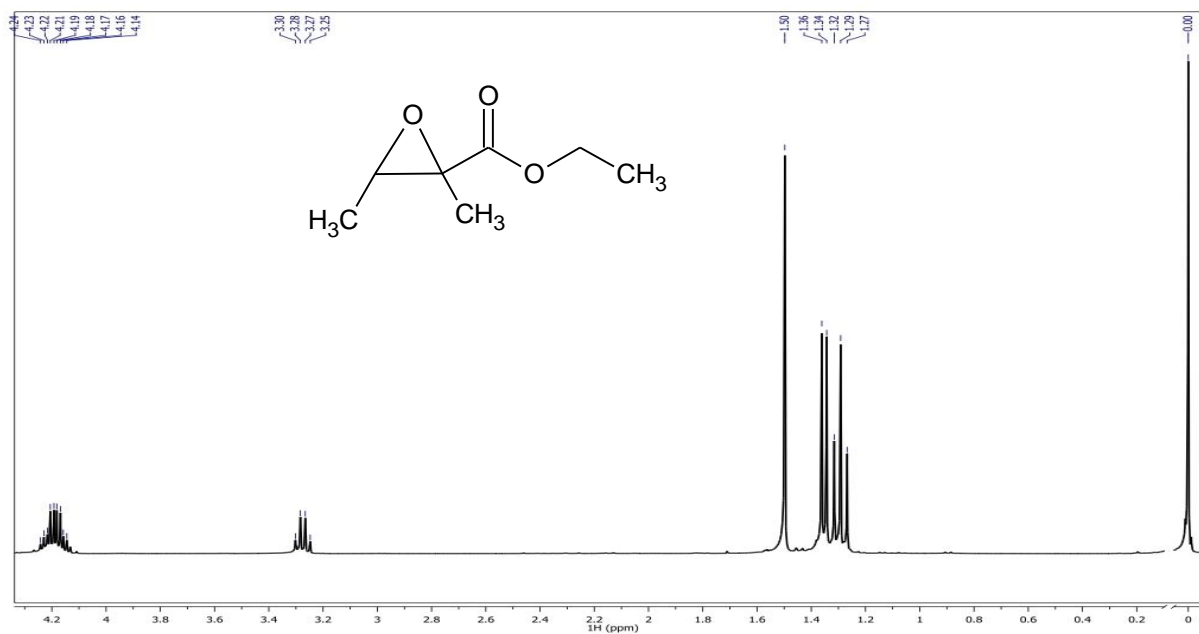
Figure 5:^{13}CNMR spectrum of ethyl tiglate **(1)** in CDCl$_3$.
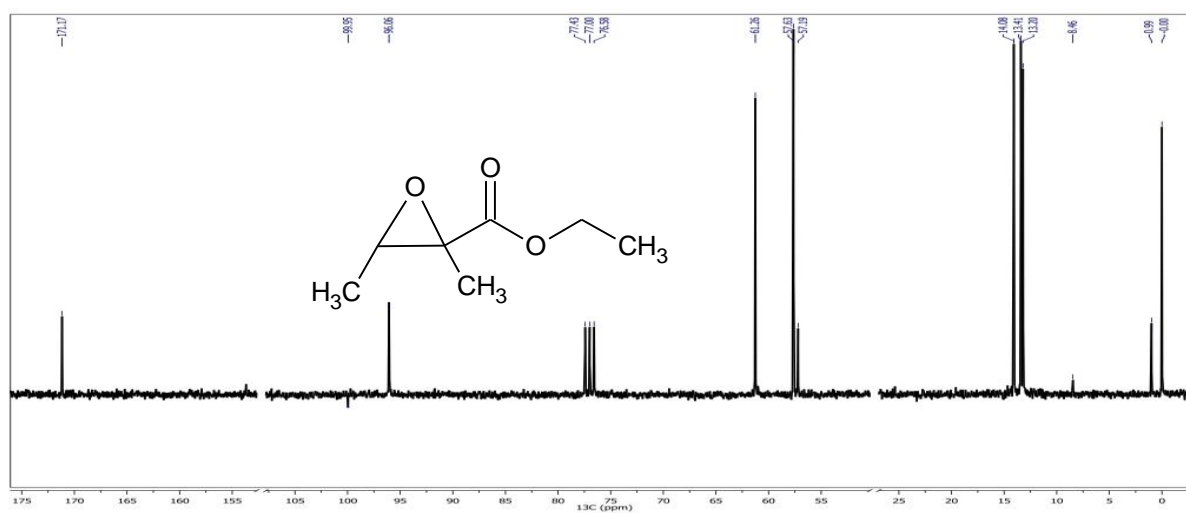
Table 5: Summary of ^{1}HNMR spectral data for epoxide product of the reaction of α,β-unsaturated ester with dimethyldioxirane in $CDCl_3/CCl_4$ solvent.

Epoxide					
1a[33]	1.29 (t,3H)	1.35 (d,3H)	1.50 (s,3H)	3.30 (q,1H)	4.20 (q,2H)
2a	1.32(d,3H)	1.55 (s,3H)	3.00 (q, 1H)	3.77 (s,3H)	
3a	1.30 (t,3H)	1.56 (s,3H)	2.70 (d,1H)	3.06 (d,1H)	4.19 (q,2H)
4a	1.31 (t,3H)	1.38 (s,3H)	1.43 (s,3H)	3.29 (s,1H)	4.24 (q, 2H)
5a[34]	1.24 (t,3H)	1.33 (d,3H)	3.05 (d,1H)	3.12 (m,1H)	4.15 (q, 2H)
6a	1.49 (s,9H)	2.17 (d,1H)	2.88 (m,1H)	3.28 (m,1H)	
7a	1.13 (t,3H)	2.14 (d,1H)	2.23 (m,2H)	4.24 (q,2H)	
8a	1.38 m,2H)	1.53 (m,2H)	1.92 (m,4H)	2.43 (m,1H)	3.74 (s,3H)
9a	1.47(m,2H)	1.69 (m,1H)	2.06 (m,1H)	2.13 (m,3H)	3.77 (s,3H)

Table 6: Summary of ^{13}CNMR spectral data for epoxide product of the reaction of α,β-unsaturated ester with dimethyldioxirane in $CDCl_3/CCl_4$ solvent.

Epoxide							
1a[34]	13.2	13.4	14.1	57.2	57.6	61.3	171.2[a]
2a[34]	13.6	19.1	51.9	59.3	59.5	170.0[a]	
3a[34]	14.0	17.4	52.5	54.0	61.2	171.0[a]	
4a[34]	14.3	18.2	24.3	59.2	59.9	61.2	168.3[a]
5a	14.1	17.1	53.7	54.1	61.2	168.8[a]	
6a[34]	27.9	30.7	45.8	47.7	82.1	168.0[a]	
7a	13.8	46.0	47.0	61.3	169.0[a]		
8a	18.9	19.2	23.8	24.1	52.1	56.4	57.5	171.2[a]
9a	19.1	26.7	27.2	52.2	62.8	63.6	169.7[a]

* absorptions with [a] correspond to carbonyl carbons

The full spectrum of each epoxide ester **2a-9a** can be found in Appendix A.

The ^{1}H or ^{13}CNMR spectral data were in agreement with literature values for esters[33,34] 1a-6a. No published values could be found for epoxides 7a-9a, so evidence for the formation of those epoxides was found by migration of vinylic proton signals upfield to a chemical shift similar to the hydrogens ascociated with the epoxide moieties in esters 1a-6a. The spectra of all epoxide esters was consistent with signals to be expected for those compounds.

In the ^{1}HNMR studies every ester showed at least one absorption expected for a hydrogen attached to a carbon attached to an oxygen in the range of 3 - 4.3 ppm for the epoxide moiety. Absorptions corresponding to hydrogens connected to carbons not directly attached to electronegative atoms were seen in the ranges of $1.1 – 2$ ppm, which is typical of these protons.

The ^{13}CNMR spectra were also consistent with expected absorptions. Every epoxide ester Had a single absorption between the ranges of $168 – 171.2$ ppm corresponding to the carbonyl carbon. The epoxide esters also all contained three absorptions in the range 45-82 ppm corresponding to carbons attached to oxygens, one for each carbon attached to the epoxide oxygen, and a third for the carbon attached at the alkoxy linkage. Each spectra also contains absorptions pertaining to CH_3 groups not attached to electronegative atoms in the range of 13-27 ppm.

B. Kinetic Experiments

The epoxidation of alkenes is known to follow a second order rate constant. The k_2 values were calculated under pseudo first order conditions with a 10:1 molar excess of ester at room temperature. The concentration of dimethyldioxirane over the course of the reaction was then

observed via UV/VIS spectroscopy. Figure 6 shows the loss of absorption of dimethyldioxirane over the course of a reaction.
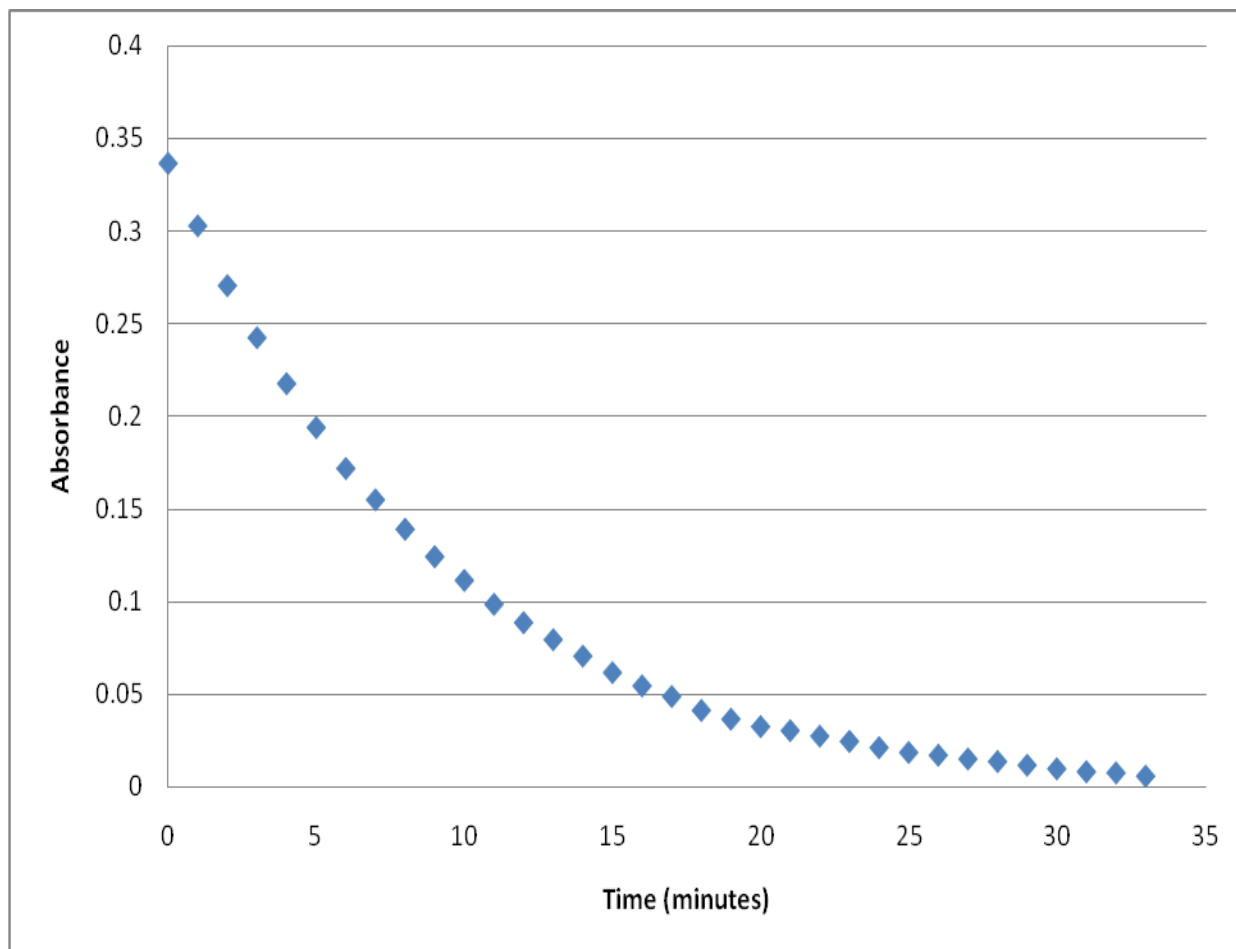
Figure 6: Absorbance of 1.0 mL of dimethyldioxirane with respect to time at 330 nm while undergoing reaction with 0.1 mL ethyl tiglate in acetone at 23^0 C.

The natural log of absorbance with respect to time is calculated and then plotted. A best fit line through the data points gives a slope of the data (Figure 7). The slope of the line is then used to calculate k_2 constants at room temperature.
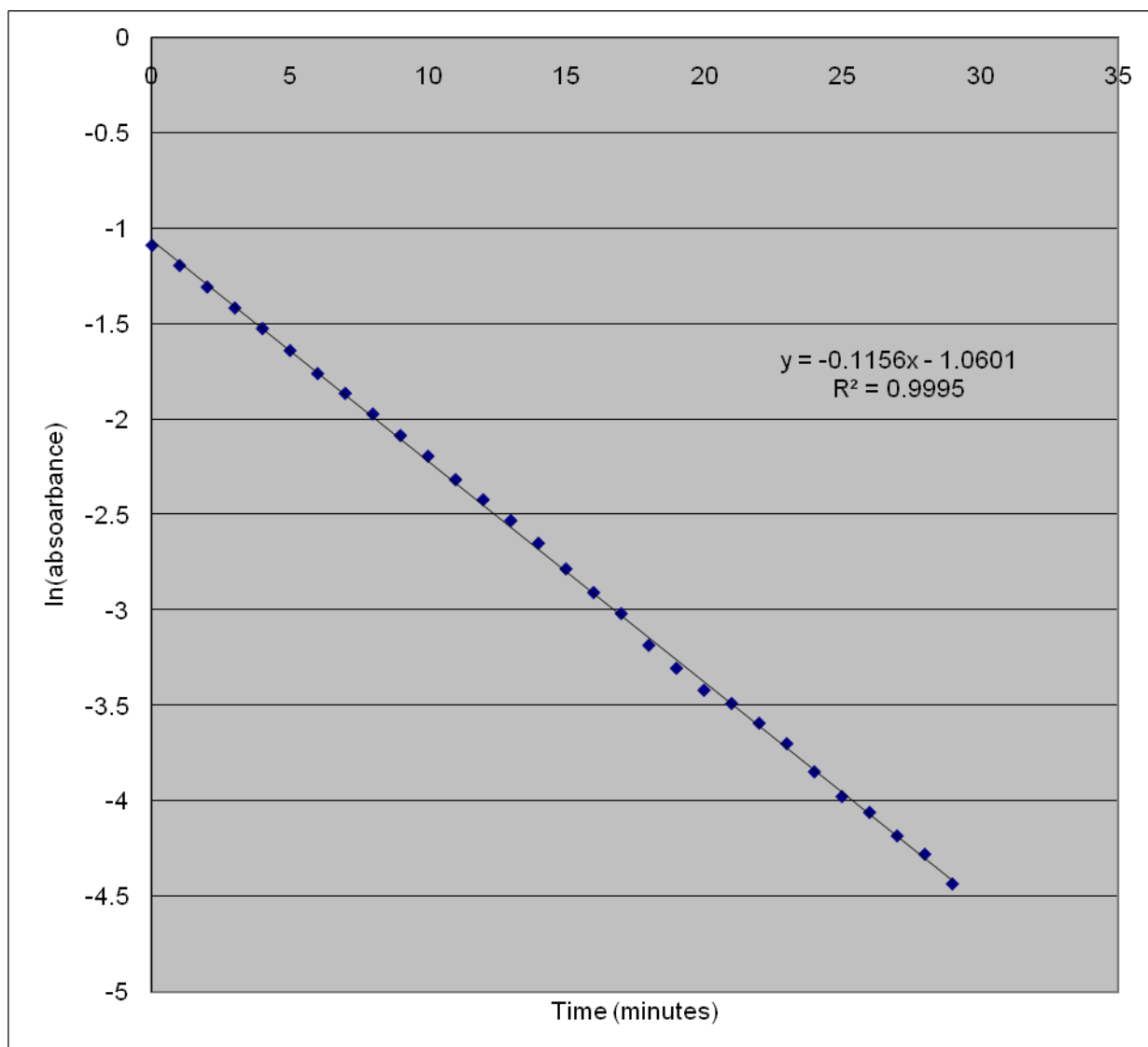
Figure 7: Natural log of Absorbance of 1.0 mL of dimethyldioxirane with respect to time at   330 nm while undergoing reaction with 0.1 mL ethyl tiglate in acetone at 23^0 C.

The reaction of dimethyldioxirane with α,β-unsaturated esters was shown to be first order with respect to both dioxirane and ester by the comparison of pseudo first order kinetic data of both a 1:10 ratio of dimethyldioxirane to angelic methyl ester, and 10:1 ratio (Appendix B). The two ratios had similar k_2 values (Table 7), suggesting that the reaction is indeed second order.

Table 7: Comparison of k_2 values of the reaction of dimethyldioxirane with angelic methyl ester at a 10:1 and 1:10 molar ratio.

Ratio of Dioxirane to Ester	Dioxirane (M)	Ester (M)	k_2 (M^{-1} s^{-1})x10^{-3}
1:10 ratio	0.03	0.27	2.04
10:1 ratio	0.1	0.014	3.00
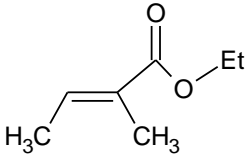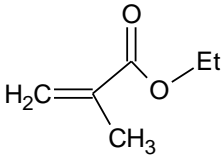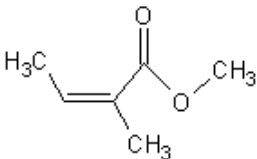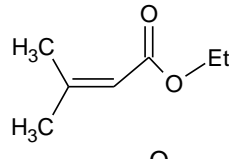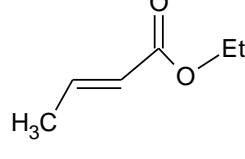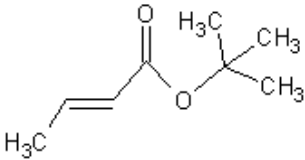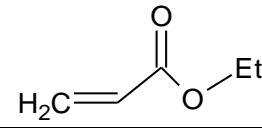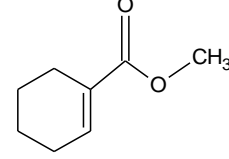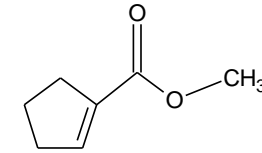
As a second check of accuracy and purity of reagents, the kinetics for each ester was run in both a more concentrated and less concentrated dilution (Appendix B), but still at a 10:1 ratio. Both the more concentrated and less concentrated dilutions gave essentially the same k_2 (Table 8).

Table 8: Comparison of concentrations and k_2 value of reaction of dimethyldioxirane with ethyl acrylate at two different dilutions.

Dimethyldioxirane (M)	Ethyl acrylate (M)	k_2 (M^{-1} s^{-1})
0.03	0.28	1.70 x 10^{-3}
0.02	0.19	1.70 x 10^{-3}
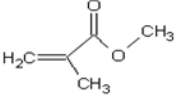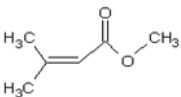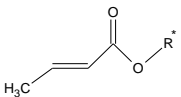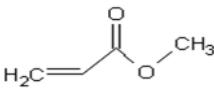
Table 9 below, shows the calculated rate constants and relative reaction rates for the epoxidation of α,β-unsaturated esters **1-9** by dimethyldioxirane in dried acetone at 23 $^{\circ}$C.

Table 9: k_2 rate constants for dimethyldioxirane with esters **1-9** at 23° C.

Ester		k_2 (M^{-1} s^{-1})*10^3	k_{rel}
1		9.6	56.5
2		2.35	13.8
3		2.0	11.7
4		1.6	9.4
5		0.35	2
6		0.27	1.6
7		0.17	1
8		6.7	1
9		14.9	2.2

The k_2 value for esters **2,4,5,** and **7** were compared to results from previous experimenters with good agreement in general except for the literature results for esters **2** and **5** which were inadvertently switched (Table 10).

Table 10: Comparison of kinetic data for epoxidation of esters **2,4,5,** and **7** by dimethyldioxirane.

Ester	Literature[18] k_2 ($M^{-1}s^{-1}$)	Unpublished senior research[35] k_2 ($M^{-1}s^{-1}$)	Experimental k_2 ($M^{-1}s^{-1}$)
2	3.9×10^{-4}	2.2×10^{-3}	2.35×10^{-3}
4	No Data	1.1×10^{-3}	1.6×10^{-3}
5	2.3×10^{-3}	3.5×10^{-4}	3.5×10^{-4}
7	No Data	1.9×10^{-4}	1.7×10^{-4}

*R= Me for Literature, R = Et for Senior research, and experimental

The unpublished senior research by Aly[35], is in good agreement with k_2 values for this body of work. The esters used for both experiments were exactly the same. If the literature k_2 values for esters 3 and five are switched[18] there is very good agreement for ester 3 (2.2, 2.3, and 2.35 $M^{-1}s^{-1}$). The k_2 values for ester 5 have a bigger difference between the literature value and the two other studies (3.9 M^{-1} s^{-1} $\times10^{-4}$ vs. 3.5 M^{-1} s^{-1} $\times10^{-4}$), which is likely due to different substituents on the alkoxy group, where the literature value was derived from the methyl ester,

and the two subsequent studies used the ethyl ester. The studies are still comparable however as

the alkoxy substituent has been shown to have little effect on the overall rate constant.

C. Computer Modeling Studies
I. Ground State Modeling

Each of the seven open chain esters was modeled using Spartan '04 in different ground

state conformations. Each ester was constrained to both an S-cis and S-trans conformation and

minimized. A third possibility of a twisted hybrid was predicted by the computer by was found to

be of much higher energy than the constrained models in every case. A ground state equilibrium

calculation was then performed on every minimized ester using the density functional method

with a 6-31G* basis set. A Gibbs free energy for each ester in each conformer was then

calculated. By subtracting the Gibbs free energy of each ground state conformer a ΔG was found

for the equilibrium between S-cis and S-trans. The difference in free energy between the

conforms was then used to predict the percentage of each conformer at room temperature. A

control calculation was carried out using the known values of the equilibrium between

cyclohexane in the chair and twist boat forms. The results were in good agreement with

experimental findings (Table 11).

Table 11: Control experiment comparing the Calculated energy difference between the chair and

twisted boat conformations of cyclohexane at the density functional level.

	E Chair (J/mol)	E Twist boat (J/mol)	ΔE calculated (J/mol)	ΔE Experimental[36] (J/mol)
Cyclohexane	-618923.851	-618901.105	22.75	23

Tables 12-20 summarize the ground state equilibrium calculations of conformers of esters **1-9**.

Table 12: Ground state energies and percentages of S-cis and S-trans conformations of methyl acrylate at room temperature using density functional calculations.

Methyl Acrylate (7)	Energy (Kcal/mol)	ΔE (Kcal/mol)	k	Percent
S-cis	-192270.634	-0.768	0.273	78.5
S-trans	-192269.866			21.5

Table 13: Ground state energies and percentages of S-cis and S-trans conformations of t-butyl crotonate at room temperature using density functional calculations.

t-Butyl Crotonate (6)	Energy (Kcal/mol)	ΔE (Kcal/mol)	k	Percent
S-cis	-290894.293	-0.597	0.365	73.3
S-trans	-290893.696			26.7

Table 14: Ground state energies and percentages of S-cis and S-trans conformations of methyl crotonate at room temperature using density functional calculations.

Methyl Crotonate (5)	Energy (Kcal/mol)	ΔE (Kcal/mol)	k	Percent
S-cis	-216929.2	-0.966	0.196	83.6
S-trans	-216928.234			16.4

Table 15: Ground state energies and percentages of S-cis and S-trans conformations of methyl 3,3-dimethyl acrylate at room temperature using density functional calculations.

Methyl 3,3Dimethyl Acrylate (4)	Energy (Kcal/mol)	ΔE (Kcal/mol)	k	Percent
S-cis	-241585.246	-1.764	0.051	95.1
S-trans	-241583.482			4.9

Table 16: Ground state energies and percentages of S-cis and S-trans conformations of methyl

methacrylate at room temperature using density functional calculations.

Methyl methacrylate (2)	Energy (Kcal/mol)	ΔE (Kcal/mol)	k	Percent
S-cis	-216926.923	0.304	0.597	37.4
S-trans	-216927.227			62.6

Table 17: Ground state energies and percentages of S-cis and S-trans conformations of angelic

methyl ester at room temperature using density functional calculations.

Angelic methyl ester (3)	Energy (Kcal/mol)	ΔE (Kcal/mol)	k	Percent
S-cis	-241582.837	-12.18	1.15E-09	100
S-trans	-241570.657			0

Table 18: Ground state energies and percentages of S-cis and S-trans conformations of tiglic

methyl ester at room temperature using density functional calculations.

Tiglic methyl ester (1)	Energy (Kcal/mol)	ΔE (Kcal/mol)	k	Percent
S-cis	-241583.914	-0.075	0.881	53.2
S-trans	-241583.839			46.8

Table 19: Ground state energies and percentages of S-cis and S-trans conformations of methyl-1-

cylohexene carboxylate at room temperature using density functional calculations.

Methyl-1-cyclohexene-1-carboxylate (8)	Energy (Kcal/mol)	ΔE (Kcal/mol)	k	Percent
S-cis	-290144.93	0.009	0.984925	49.5
S-trans	-290144.939			50.5

Table 20:Ground state energies and percentages of S-cis and S-trans conformations of methyl-1-cyclopentene carboxylate at room temperature using density functional calculations

Methyl-1-cyclopentene-1-carboxylate **(9)**	Energy (Kcal/mol)	ΔE (Kcal/mol)	k	Percent
S-cis	-265488.359	0.15	0.776335	43.7
S-trans	-265488.509			56.3

II. Transition State Modeling

A transition state calculation was carried out on each ester in both the S-cis and S-trans conformation, except in the cases of angelic methyl ester and methyl 3,3-dimethyl acrylate which do not have significant concentrations of the S-trans isomer at room temperature. Two transition state models were carried out for each ester conformer relating to the two faces of attack of dimethyldioxirane described as "in" and "out", where "in" describes the methyl groups of the dioxirane positioned over the carbonyl group, or in the plane of the molecule, and "out" describes the 180 degree flip of that. Methyl esters were used in all cases to simplify the calculations, and minimize errors that may be derived from rotation of an ethoxy group, and comparison of the energy of a methyl group vs. that of an ethyl group. Each transition state energy was used along with the ground state calculations and a ground state energy calculation of dimethyldioxirane to find the energy of activation of the reaction. Calculations were first undertaken using a semi empirical approach using the AM-1 method where the heat of formation of the starting materials, transition state, and dimethyldioxirane were used to calculate the energy of activation at 23° C. (Tables 21-27).

Table 21: Ground state, transition state, and activation energies for the reaction of methyl

acrylate with dimethyldioxirane using the AM-1 method.

Methyl acrylate (6)	Ground state energy (Kcal/mol)	Transition state energy In (Kcal/mol)	Transition state energy Out. (Kcal/mol)	Ea in (Kcal/mol)	Ea out (Kcal/mol)
S-cis	-69.616	-40.04	-39.479	18.868	19.429
S-trans	-70.037	-39.477	-39.292	19.852	20.037

Table 22: Ground state, transition state, and activation energies for the reaction of methyl

crotonate with dimethyldioxirane using the AM-1 method.

Methyl crotonate (5)	Ground state energy (Kcal/mol)	Transition state energy In (Kcal/mol)	Transition state energy Out. (Kcal/mol)	Ea In (Kcal/mol)	Ea Out (Kcal/mol)
S-cis	-80.574	-49.406	-48.897	20.46	20.969
S-trans	-80.138	-48.82	-48.728	20.61	20.702

Table 23: Ground state, transition state, and activation energies for the reaction of methyl 3,3-

dimethyl acrylate with dimethyldioxirane using the AM-1 method.

Methyl 3,3 dimethyl acrylate (4)	Ground state energy (Kcal/mol)	Transition state energy In (Kcal/mol)	Transition state energy Out. (Kcal/mol)	Ea In (Kcal/mol)	Ea Out (Kcal/mol)
S-cis	-86.445	-56.486	-56.299	19.438	19.438

Table 24: Ground state, transition state, and activation energies for the reaction of methyl methacrylate with dimethyldioxirane using the AM-1 method.

Methyl methacrylate (2)	Ground state energy (Kcal/mol)	Transition state energy In (Kcal/mol)	Transition state energy Out. (Kcal/mol)	Ea In (Kcal/mol)	Ea Out (Kcal/mol)
S-trans	-76.530	-45.959	-45.397	19.863	20.425
S-cis	-76.642	-46.303	-45.309	19.631	20.625

Table 25: Ground state, transition state, and activation energies for the reaction of angelic methyl ester with dimethyldioxirane using the AM-1 method.

Angelic methyl ester (3)	Ground state energy (Kcal/mol)	Transition state energy In (Kcal/mol)	Transition state energy Out. (Kcal/mol)	Ea In (Kcal/mol)	Ea Out (Kcal/mol)
S-cis	-85.48	-52.667	-52.514	22.105	22.258

Table 26: Ground state, transition state, and activation energies for the reaction of tiglic methyl ester with dimethyldioxirane using the AM-1 method.

Tiglic methyl ester (1)	Ground state energy (Kcal/mol)	Transition state energy In. (Kcal/mol)	Transition state energy Out. (Kcal/mol)	Ea in (Kcal/mol)	Ea out (Kcal/mol)
S-cis	-85.819	-53.757	-52.35	21.354	22.761
S-trans	-85.596	-52.751	-52.795	22.137	22.093

Table 27: Ground state, transition state, and activation energies for the reaction of 1-methyl cyclohexene carboxylate with dimethyldioxirane using the AM-1 method.

Methyl- 1 - cyclohexene-1- carboxylate (8)	Ground state energy (Kcal/mol)	Transition state energy In. (Kcal/mol)	Transition state energy Out. (Kcal/mol)	Ea In (Kcal/mol)	Ea Out (Kcal/mol)
S-trans	-93.945	-59.775	-61.037	23.726	22.2
S-cis	-93.945	-59.511	-61.236	23.462	22.001

Table 28: Ground state, transition state, and activation energies for the reaction of 1-methyl

cyclopentene carboxylate with dimethyldioxirane using the AM-1 method.

Methyl -1-cyclopentene-1-carboxylate (9)	Ground state energy (Kcal/mol)	Transition state energy In (Kcal/mol)	Transition state energy out (K/cal/mol)	Ea In (Kcal/mol)	Ea out (Kcal/mol)
S-cis	-81.091	-47.19	-48.283	23.193	22.100
S-trans	-81.059	-48.068	-46.923	22.283	23.428

The transition state calculations were also carried out using the density functional level with a

6-31 G* basis set to compare to the semi-empirical calculations (Tables 29-36).

Table 29: Ground state, transition state, and activation energies for the reaction of methyl

acrylate with dimethyldioxirane using the density functional method.

Methyl acrylate (7)	Ground state energy (Kcal/mol)	Transition state energy In. (Kcal/mol)	Transition state energy Out. (Kcal/mol)	Ea In (Kcal/mol)	Ea Out (Kcal/mol)
S-cis	-192270.634	-360544.3	-360543.281	29.31	30.348
S-trans	-192269.866	-360542.6	-360542.932	30.246	29.929

Table 30: Ground state, transition state, and activation energies for the reaction of methyl

crotonate with dimethyldioxirane using the density functional method.

Methyl crotonate (5)	Ground state energy (Kcal/mol)	Transition state energy In. (Kcal/mol)	Transition state energy Out. (Kcal/mol)	Ea In (Kcal/mol)	Ea Out (Kcal/mol)
S-cis	-216929.2	-385203.117	-385200.316	29.078	31.879
S-trans	-216928.234	-385201.584	-385200.067	29.645	31.162

Table 31: Ground state, transition state, and activation energies for the reaction of methyl 3,3-

dimethyl acrylate with dimethyldioxirane using the density functional method.

Methyl 3,3-dimethyl acrylate (**4**)	Ground state energy (Kcal/mol)	Transition state energy In. (Kcal/mol)	Transition state energy Out. (Kcal/mol)	Ea In (Kcal/mol)	Ea Out (Kcal/mol)
S-cis	-241585.246	-409857.475	-409858.204	30.766	30.037

Table 32: Ground state, transition state, and activation energies for the reaction of methyl

methacrylate with dimethyldioxirane using the density functional method.

Methyl methacrylate (**2**)	Ground state energy (Kcal/mol)	Transition state energy In. (Kcal/mol)	Transition state energy Out. (Kcal/mol)	Ea In (Kcal/mol)	Ea out (Kcal/mol)
S-trans	-216927.227	-385201.566	-385200.818	28.656	29.404
S-cis	-216926.923	-385202.149	-385199.912	27.769	30.006

Table 33: Ground state, transition state, and activation energies for the reaction of angelic

methyl ester with dimethyldioxirane using the density functional method.

Angelic methyl ester (**3**)	Ground state energy (Kcal/mol)	Transition state energy In. (Kcal/mol)	Transition state energy Out. (Kcal/mol)	Ea In (Kcal/mol)	Ea Out (Kcal/mol)
S-cis	-241582.837	-409855.558	-409856.302	30.274	29.53

Table 34: Ground state, transition state, and activation energies for the reaction of tiglic methyl

ester with dimethyldioxirane using the density functional method.

Tiglic methyl ester (**1**)	Ground state energy (Kcal/mol)	Transition state energy In. (Kcal/mol)	Transition state energy Out. (Kcal/mol)	Ea In. (Kcal/mol)	Ea Out (Kcal/mol)
S-Cis	-241583.914	-409859.8	-409855.149	27.081	31.760
S-trans	-241583.839	-409858.8	-409855.402	28.04	31.432

Table 35: Ground state, transition state, and activation energies for the reaction of 1-methyl cyclohexene carboxylate with dimethyldioxirane using the density functional method.

Methyl-1-cyclohexene-1-carboxylate (8)	Ground state energy (Kcal/mol)	Transition state energy In. (Kcal/mol)	Transition state energy Out. (Kcal/mol)	Ea In (Kcal/mol)	Ea Out (Kcal/mol)
S-trans	-290144.939	-458414.1	-458419.574	33.834	28.36
S-cis	-290144.93	-458420.279	-458420.865	34.114	27.06

Table 36: Ground state, transition state, and activation energies for the reaction of 1-methyl cyclopentene carboxylate with dimethyldioxirane using the density functional method.

Methyl -1-cyclopentene -1-carboxylate (9)	Ground state energy (Kcal/mol)	Transition state energy In. (Kcal/mol)	Transition state energy Out. (Kcal/mol)	Ea In (Kcal/mol)	Ea Out (Kcal/mol)
S-trans	-265488.509	-433760.19	-433764.049	31.314	27.455
S-cis	-265488.359	-433758.983	-433764.804	32.371	26.55

All calculations done at the density functional level were subject to additional IR spectrum calculations. All transition state calculations at the density functional level yielded a single imaginary IR absorption between $500 – 2000 \text{ cm}^{-1}$, suggesting that the transition states were all in a local minimum of energy. Animation of the motion of ascociated with the absorption shows stretching of the new C-O-C bond and breaking O-O bond. Table 37 summarizes the differences in activation energy found via semi-emperical AM1 modeling and calculations using the density functional approach.

Table 37: Summary of the energy of activation calculated for the reaction of each ester with dimethyldioxirane using both the AM-1 and density functional methods.

Ester	Lowest Ea AM1 (Kcal/mol)	Lowest Ea Density Functional (Kcal/mol)
Methyl acrylate (7)	18.868	29.310
Methyl crotonate (5)	20.460	29.078
Methyl 3,3-dimethyl acrylate (4)	19.438	30.037
Angelic methyl ester (3)	22.105	29.530
Methyl methacrylate (2)	19.631	27.769
Tiglic methyl ester (1)	21.354	27.081
1-Methyl cyclohexene Carboxylate (9)	22.001	27.060
1-Methyl cyclopentene carboxylate (8)	22.283	26.550

III. Relative k₂ Determination

The energy of activation of each ester with dimethyldioxirane was used to calculate relative k_2 values. The energy of activation of each reaction is proportional to the relative k value by the equation $e^{(\Delta Ea/RT)}$. A simple control test was done to ensure that accurate relative k_2 values could be found. The well studied cis and trans 2-butene were modeled using the density functional method and compared to literature values (Table 38).
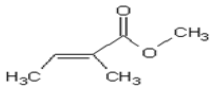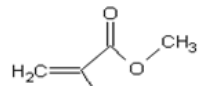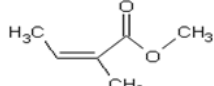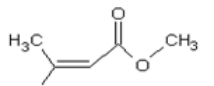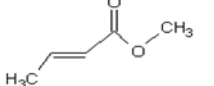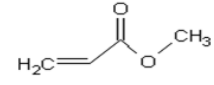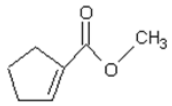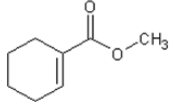
Table 38: Calculation of the relative k_2 value of the reaction of trans and cis 2-butene with dimethyldioxirane using the density functional method

	Transition State energy (Kcal/mol)	Ground State Energy (Kcal/mol)	ΔE (Kcal/mol)	literature value[37] ΔE (Kcal/mol)
trans-2-butene	-266885.996	-98610.1152	1.35	1.7
cis-2-butene	-266886.438	-98609.202		

The calculated relative k_2 value found was in good agreement with the literature value[37] and gives a relative k value closer to experimental results than the previous literature, so the same method was followed for calculation of relative k_2 values of the nine α,β-unsaturated esters.
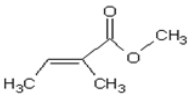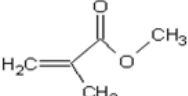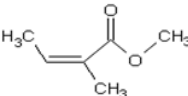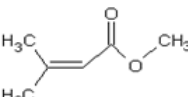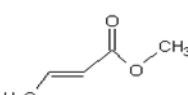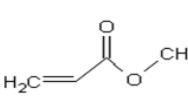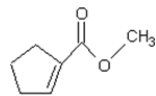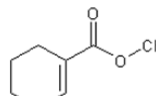
The relative rate constants were calculated using both the lowest activation energy found for each ester using both the AM-1(Table 39) and density functional (Table 40) methods, and a weighted average of conformers is summarized below.

Table 39: Comparison of experimentally determined relative k_2 values to calculated k_2 values using the AM-1 method.

Ester		Experimental $k_{2\,rel}$	Calculated $k_{2\,rel}$	Calculated $k_{2\,rel}$ weighted average
1		56.5	0.015	0.012
2		13.8	0.004	0.006
3		11.7	0.276	0.309
4		9.4	0.354	0.506
5		2.0	0.068	0.093
7		1.00	1.00	1.00
8		2.2	0.92	0.84
9		1.00	1.00	1.00

* The modeling for t-butyl crotonate was left out due to its differing alkoxy group. The data for this model can be found in Appendix C.

Table 40: Comparison of experimentally determined relative k_2 values to calculated k_2 values using the density functional method.

Ester		Experimental k_2 rel	Calculated $k_{2\,rel}$	Calculated $k_{2\,rel}$ weighted average
1		56.5	42.84	25.63
2		13.8	13.36	10.12
3		11.7	0.29	0.29
4		9.4	0.69	0.69
5		2.0	1.47	1.58
7		1.00	1.00	1.00
8		2.2	2.37	3.03
9		1.00	1.00	1.00

* The modeling for t-butyl crotonate was left out due to its differing alkoxy group. The data for this model can be found in Appendix C.

The relative reactivity of esters **3** and **4** were not correctly predicted by the computer model using the density functional method. A closer look at the geometry of the transition states of these two esters compared to that of esters **7** and **2** shows some fundamental differences in the

transition states (Table 41). A rotation angle for each ester with dioxirane was measured by defining a plane through the central carbon and the two oxygens of dioxirane, as well as a second plane through the two carbons of the alkene of the ester with the incoming oxygen. In a true butterfly transition state this angle would be measured to be 90 degrees. A second angle was defind as "tilt", which describes the angle between a plane defined by the three carbons of dioxirane, and a second plane defined by the two carbons of the alkene and neighboring carbon. A tilt of 0 degrees would show the dioxirane to be flat relative to the ester in the transition state.

Table 41: Measured angles of the transition states of esters **2,3,4 and 7**.

Compound	Rotation angle (Deg)	Tilt angle (Deg)
Methyl 3,3-dimethyl Acrylate **(4)**	82.72	9.60
Angelic Methyl ester **(3)**	89.91	10.61
Methyl Acrylate **(7)**	80.86	27.02
Methyl Methacrylate **(2)**	87.16	23.83

Methods

A. Dimethyldioxirane Synthesis

Dioxirane was prepared by the reaction of 2-propanone (acetone) with potassium monoperoxysulfate (oxone) using a modified procedure from the one by Murray[13]. Glassware was pretreated with boiling 1% disodium ethylidene tetra-aminoacid (Na$_2$EDTA) (Fischer Scientific, ACS certified) in dionized water, then rinsed with acetone (Sigma-Aldrich, HPLC grade) and dried. To a 3 liter, 3 neck round bottom flask, 96 grams of Sodium Bicarbonate (NaHCO$_3$) (Fischer Scientific, ACS certified) and 1.5 grams of Na$_2$EDTA were added. A mixture of 80 mL acetone and 60 mL DI water was then added to the flask, and stirred via mechanical stirrer. A second mixture of H$_2$0/Acetone (80 mL/53 mL) was added drop wise via a pressure equalizing funnel, at the same time as 200 g Oxone (Sigma-Aldrich) were being added via a pressure equalizing powder-addition-funnel, over the course of thirty minutes. The dioxirane was collected as an acetone solution in a receiving trap cooled to -78˚ C by a mixture of dry ice and acetone, under reduced pressure over the course of one hour. The dioxirane was then distilled under reduced pressure at -20˚ C in order to remove water and to concentrate the solution. The final solution was stored over anhydrous Na$_2$SO$_4$ at -20˚ C. The final dioxirane/acetone solutions were found to be between 0.08 and 0.1 M.

B. Kinetic Experiments

Second-order kinetics were determined under pseudo-first order conditions of either 10:1, or 1:10 molar ratio of ester to dioxirane. trans-Eylcrotonate, ethyl methacrylate, and ethyl acrylate were obtained from Aldrich (Sigma-Aldrich) with 99% purity. Ethyl-3,3-dimethyl acrylate, and t-

Butyl acrylate were obtained from Alrich (Sigma-Aldrich) with 98% purity. Methyl-1-cyclohexen-1-carboxylate and methyl-1-cyclopentene-1-carboxylate were obtained from Sigma-Aldrich with 97+% purity. Angelic methyl ester, and ethyl tiglate were obtained from TCI America in 97% and 99% purity respectively. The purity of the esters was checked by GC/MS (Shimadzu GC17-A Gas Chromatograph coupled to a Shimadzu QP-5000 MS Spectrometer). The dioxirane solution and the ester were added to a 3 ml quartz cuvette in a 1:10 ratio and diluted to a total volume of 3 ml with dried acetone. Disappearance of the dioxirane was monitored via UV/Vis spectroscopy at 330 nm, on a Shimadzu UV1601 spectrophotometer. The temperature of the cell was kept at 23 +/- 0.3 $^{\circ}$C with an attached water jacket and constantly circulating water bath (Haake-K water bath). The temperature of the bath was measured using a YSI Model 42SC Tele-Thermometer. A final baseline was established by addition of 2,3-dimethyl-2-butene (Sigma-Aldrich) after the reaction had gone to completion to insure no residual dioxirane was absorbing. The pseudo-first order rate values were then calculated using Microsoft Excel. The second order rate constants were calculated the usual way by dividing the observed rate by the molar concentration of the reactant in excess.

C. Product Studies

The products of the reaction of dimethyldioxirane and the esters were established by ^{1}HNMR and ^{13}C NMR spectroscopy. As an example, the reaction of 0.025 ml of pure ester **1** with 7 ml of dioxirane/acetone solution was allowed to go to completion in a round bottom flask, at room temperature, in a dark vessel. When the reaction was completed, up to 12 ml of carbon tetrachloride (Sigma-Aldrich) were then added to the flask. The acetone and most of the carbon

tetrachloride was removed by short-path microdistillation, down to roughly 0.7 ml total volume. Tetramethylsilane (0.03%) in $CDCl_3$ (Sigma-Aldrich) was then added to the residual volume in the distillation flask. The ^1H NMR and ^{13}C NMR spectra of the samples were then obtained on a 300 MHZ Varian INOVA NMR or a 400 MHZ Bruker NMR.   The spectra obtained were, when available, compared to the literature values.

D. Computer Modeling Studies

Computer modeling studies of the transition state of each α,β-unsaturated ester with dimethyldioxirane were done using Spartan '04 (Wavefunctions inc.). Past transition state studies using the AM1 approach have showed excellent correlation to experimentally determined kinetics values[11]. Semi empirical methods have been used to accurately describe alkene and sulfide oxidations among others[12,13]. A study of α,β-unsaturated ketones by Chen found that the AM1 approach was insufficient to describe the reaction, likely due to differences in the electron density of the ester throughout the reaction[18]. Density functional modeling studies with a 6-31G* basis set were shown to be more accurate in describing the α,β-unsaturated ketones and hence were applied to α,β-unsaturated esters for this study. Each reagent was minimized separately then merged with no further geometry optimization. The equilibrium geometry of each ground state ester was calculated in a vacuum in several conformations predicted by Spartan to examine whether they are mostly in a S-cis, S-trans or some twisted hybrid at equilibrium. The reagents were then positioned manually into a spiro transition state attacking from each side of the alkene and the flow of electrons was input into the program (Figure 8).
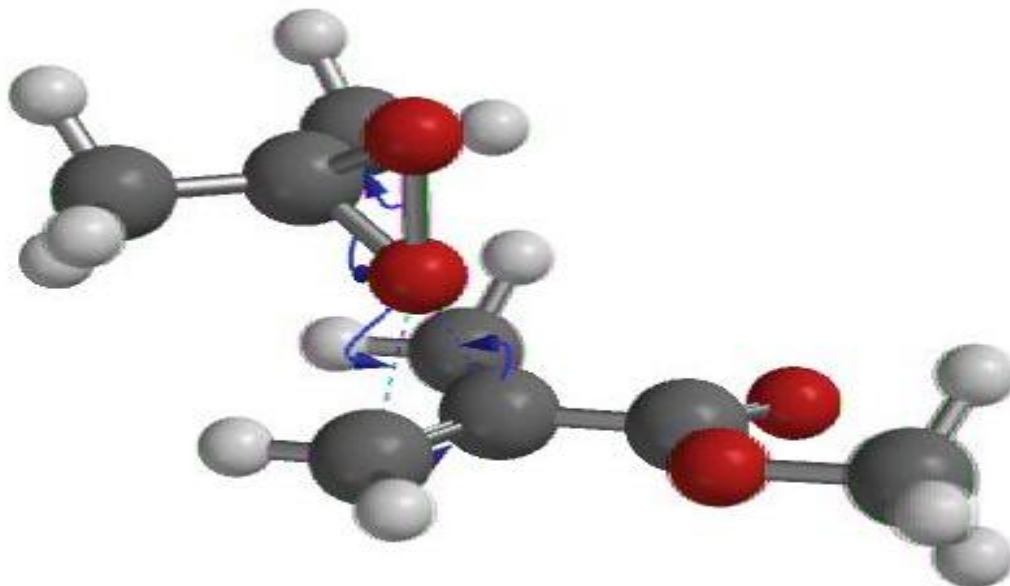
Figure 8: The flow of electrons as input into Spartan to calculate the optimum geometery of the transition state of methyl methacrylate with dimethyldioxirane.

Pressing the [⟳] button then brings up a guess at the transition state were the reagents are held in a loose association, and bond breakages and formations are shown. The transition state was calculated where the methyl groups of the dioxirane were either over the carbonyl or rotated 180 degrees away, as well as with each ester geometry found to contribute significantly to the ester at room temperature . Some transition states were also calculated with a starting planar geometry which was rearranged to the spiro state in all cases by the geometry optimization. Using the AM-1 approach the heat of formation of the ground state ester, transition state, and dimethyldioxirane were calculated for each ester. The following equations can then be applied to find the relative k_2 value.

$Ea = H_f$ transition state $- (H_f$ ground state $+ H_f$ dioxirane)

k_2 rel is proportional to $e^{(-Ea/RT)}$

Where R is the universal gas constant (R $= 1.987192$ cal K^{-1} moles^{-1})

Using the density functional approach the infrared spectrum and vibrational modes boxes must be checked in order to correct for vibrational, rotational, and translational energy at room temperature, as well as to explore the validity of the transition state through a calculated IR spectrum. After running the calculation the spreadsheet function can be opened and a ΔG value displayed. The relative rate constants can then be found by the following equations.

$Ea = \Delta G$ transition state $- (\Delta G$ ground state ester $+ \Delta G$ dioxirane)

K_2 rel is proportional to $e^{(\Delta Ea/RT)}$

where R is the universal gas constant. (R$=1.987192$ cal K^{-1} moles^{-1})

 The vibrational spectrum of each transition state complex showed a single imaginary value corresponding to a local minimum in energy along the reaction coordinate. Animation of the imaginary vibrational mode correlates to vibration of the new C-O-C bond.

Conclusions

- Nine α,β-unsaturated esters underwent complete epoxidation with no rearrangement or unexpected side reactions.

- k_2 values were determined for a series of α,β-unsaturated esters with different electron densities and steric constraints around the alkene moiety.

- The cis like ethyl tiglate underwent reaction four times faster than the trans like angelic methyl ester. This was a marked decrease in selectivity from simple alkenes.

- The germinal substituted methyl methacrylate underwent reaction faster than than 3,3-dimethyl acrylate, and angelic methyl ester both of which have a higher level of substitution.

- An error was found in previous literature were the published k_2 values for methyl methacrylate and ethyl trans crotonate were switched.

- Among the cyclic α,β-unsaturated esters the more energetic cyclopentene ring was found to undergo epoxidation more than twice as fast as the cyclohexene ring.

- Computer modeling was used to determine the ground state configuration of the nine esters and predict the percentages of each in the S-cis and S-trans configuration.

- Every ester except methyl methacrylate preferred the S-cis ground state or were found in a relatively equal distribution between S-cis and S-trans.

- The AM-1 approach to transition state modeling was found to be inadequate to calculate relative kinetics values of open chain α,β-unsaturated esters. A conclusion supported by a past study of α,β-unsaturated ketones.

- The density functional approach was adequate to predict the relative reactivity of six of the eight esters (t-butyl not used).

- The two esters that were not correctly predicted had a commonality in that they were the only two with a substituent in the R1 position.

- The model predicted the S-cis in geometry to be the lowest energy transition state for the six esters that were correctly predicted.

- Angelic methyl ester and ethyl 3,3-dimethyl acrylate show a possible steric interaction in the S-cis in geometry between the R1 methyl and methyl groups of dimethyldioxirane.

- The anomalous ethyl methacrylate reactivity is possibly linked to the differences in the ground state conformation found in this study, but raises more questions since it is more often in the S-trans conformation, which the computer predicted to be unfavorable to dioxirane attack.

- A direct visual comparison of the S-cis transition state between angelic methyl ester and tiglic methyl ester shows the steric interaction mentioned above (figures 9 -10).

- A closer study of the geometry of the transition states between the esters that were not correctly modeled by the computer and those that were, showed relatively large differences in the tilt angle. The large differences in geometry invalidate the subtraction method used to compare the energies of the transition states and lead to incomparable results.
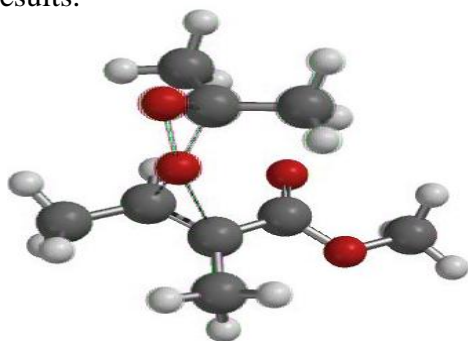

Figure 9: Tiglic methyl ester "S-cis in"   Figure 10: Angelic methyl ester "S-cis in"
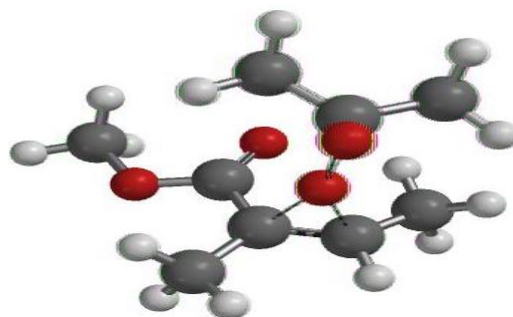
References

1. Curci, R., Gandolfi, R., Fusco, C., Dinoi, A., D'acculti, L., Annese, C,; Journal of the American Chemical Society. **2008**. 130, 1197-1204

2. Murray, R; Chemical Reviews. **1989.** 89, 1187-1201

3. Baeyer, A., Villager, V.; Ber. **1899**. 32, 3625.

4. Talbott, R., Thompson, P. US patent 632 606. **1972**

5. Martinez, R., Kafaki, A., Herron, J.; Molecular Structure and Energetics.

6. Suenram, R., Lovas, F.; Journal of the American Chemical Society. **1978.** 100 (16) 5117-5121

7. Curci, R., Fiorentino, M., Troisi, L.; Journal of Organic Chemistry. **1980**. 45, 4758-5760.

8. Murray, R.; Chemical Reviews. **1989.** 89, 1192

9. Baumstark, A., Michelena-Baez, E., Navarro, A., Banks, H.; Heterocyclic Communications. **1997**. 3 (5) 393-396

10. Baumstark, A., Chen, H., Singh, S., Vasquez, P.; Heterocyclic Communications. **1997.** 3, (5) 501-504

11. Hanson, P., Henjrickx, R., Smith, J.; Organic and Biomolecular Chemistry. **2007**. (6) 762- 771

12. Baumstark, A., Vasquez, P., Kovac, F.; Canadian Journal of Chemistry. **1999**. 77 (3) 308-312

13. Murray, R., Jeyaraman, R.; Journal of Organic Chemistry. **1985.** 50 2847-2853

14. Baumstark, A,. Vasquez, P.; Heterocyclic Communications. **2007**. 13, (1) 25-28

15. Grabovskiy, S., Timerghazin, Q., Kabal, N.; Russian Chemical Bulletin. **2005**. 54 (10) 2384-2393

16.   Adam, W., Curci, R., D'accolti, L., Dinoi, A., Fusco, C.,Gasparinni, F., Kluge, R.,

        Paredes, R., Schulze, M., Smerz, A., Veloza, L., Weinkotz, S., Winde, R.; European

        Journal of Chemistry. **1997.** 3, (1) 105-109.

17.   Fokin, A., Boryslav, A., Pavel, A., Schriener, P.; Chemistry- A European Journal. **2005**.

        11, (23) 7091-7101

18.   Han, K., Huang, G., Zhang, J., Zhang, Z.; Zhongguo Zoazhi Xuebao. **1999.** 14, 56-63

19.   Baumstark, A., Michelena-Baez, E., Navarro, A., Banks, H.; Heterocyclic

        Communications. **2000**. 6 (2) 119-122

20.   Chen, H., Ph.D. Dissertation (2001), Department of Chemistry, Georgia State

         University, Atlanta, Georgia.

21.   Navarro, A., Ph.D. Dissertation (2003), Department of Chemistry, Georgia State

        University, Atlanta Georgia

22.   Baumstark, A., Vasquez, P., Franklin, P., Cunninhgham, A.; Heterocyclic

        Communications. **1998**. 4 (3) 201- 204.

23.   Baumstark, A., Vasquez, P., Heterocyclic Communications. **2008**. 14, (1,2) 11-14

24.   Murray, R.; Shiang, D. Journal of the Chemical Society.: Perkins Transactions 2. **1990**,

        349-352.

25.   Duebel, D. Journal of Organic Chemistry. **2001**. 66, 3790-3796.

26.   Curci, R., Annise, C., D'Acculti, L., Dinoi, A., Fusco, C., Gandolfi, R.; Journal of the

        American Chemical Society. **2007**, 130, 1197-1204.

27.   Curci, R., Dinoi, A., Rubino, M.; Pure and Applied Chemistry. **1995**. 67, (5) 811-822.

28.   Giamalva, D., Church, D., Pryor, W. Journal of Organic Chemistry. **1988**. 53, 3429

29.   Curci, R., Dinoi, A., Fusco, C., Lilio, M. Tetrahedron Letters. **1995**. 37, (2) 249-252.

30. Freccero, M.,Gandolfi, R., Sarzi-Amade, M., Rastelli, A.; Tetrahedron Letters. **2001**, 42, (14), 2739-2742.

31. Kim, S., Schaefer, H. Journal of Physical Chemistry. **2000**. 104, 7892-7897.

32. McCloskey, C., Baumstark, A.; Tetrahedron Letters. **1987.** 28, 3311

33. Hadjiarapoglou, L.; Adam, W.; Nestler, B., Tetrahedron Letters, 1990, 31, 331.

34. Y.; Sanner, C.; Larcheveque, M., Synthesis, 1988, 538.

35. Aly, M.; Senior Research. Georgia State University, Dept. of Chemistry, Summer 2006.

36. Murray, R., Organic Chemistry. **2007**.

37. Jenson, C., Lui, J., Houk, K., Jourgenon, W.; Journal of the American Chemical Society. **1997.** 119, 12982-12983

Appendix A:^{1}HNMR and ^{13}CNMR spectra of epoxide products

1. ^{1}H NMR spectrum of ethyl methacrylate epoxide in CDCl$_3$.
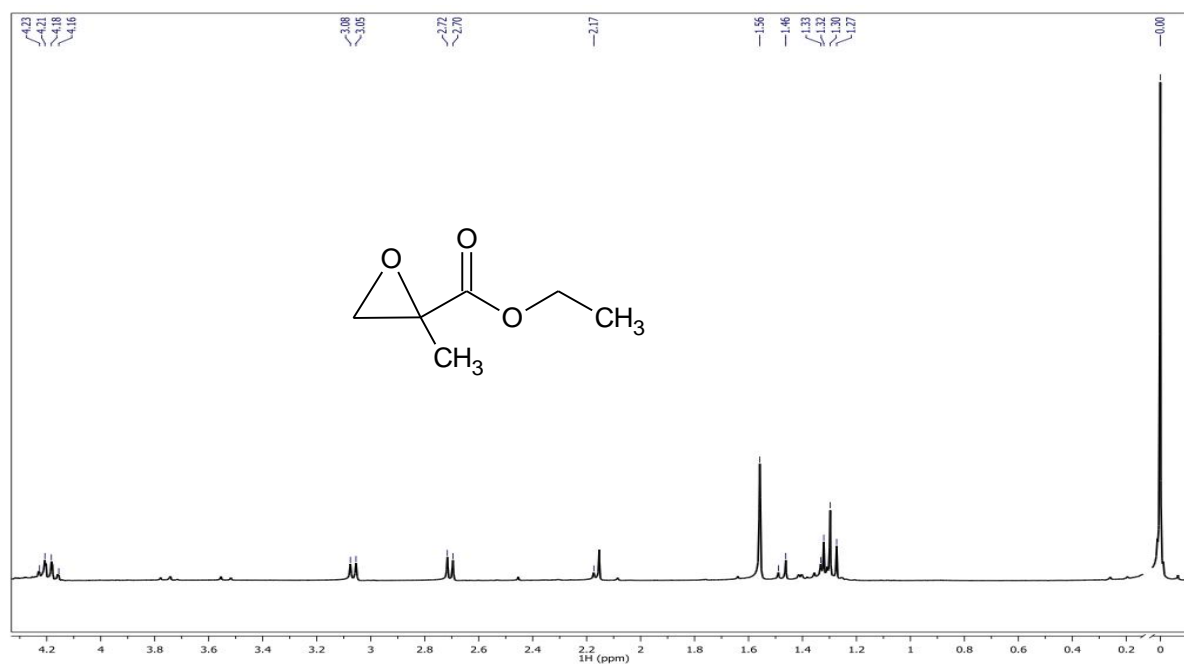
2. ^{1}H NMR spectrum of angelic methyl ester epoxide in CDCl$_3$.
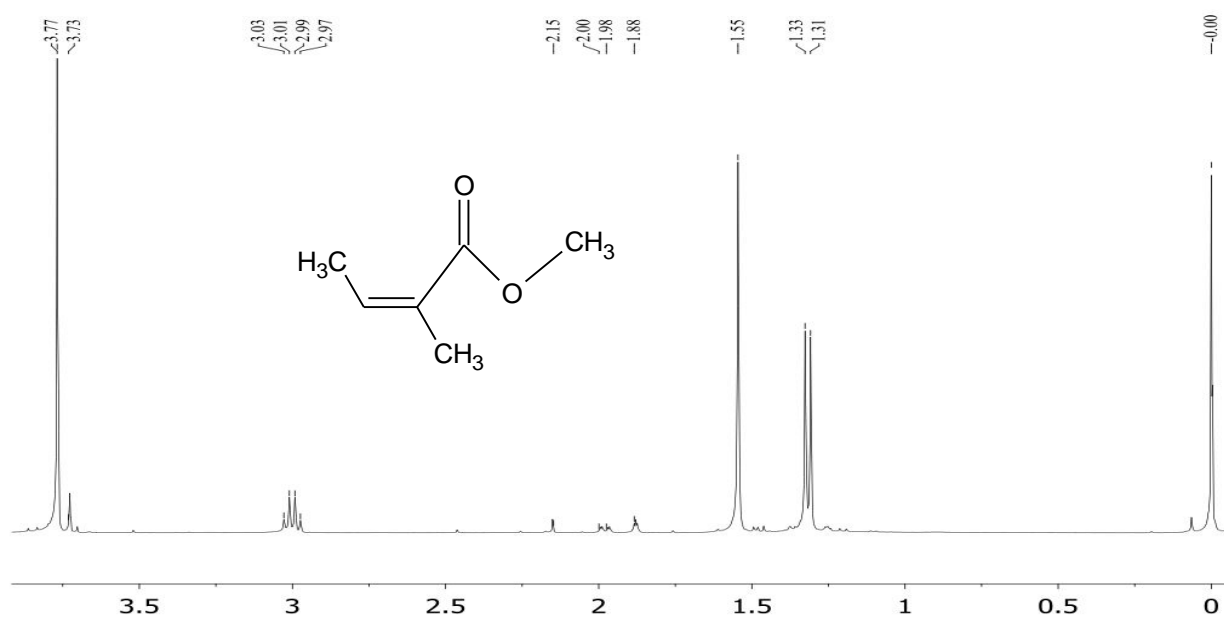
3. ^{1}H NMR spectrum of ethyl 3,3-dimethylacrylate epoxide in CDCl$_3$.
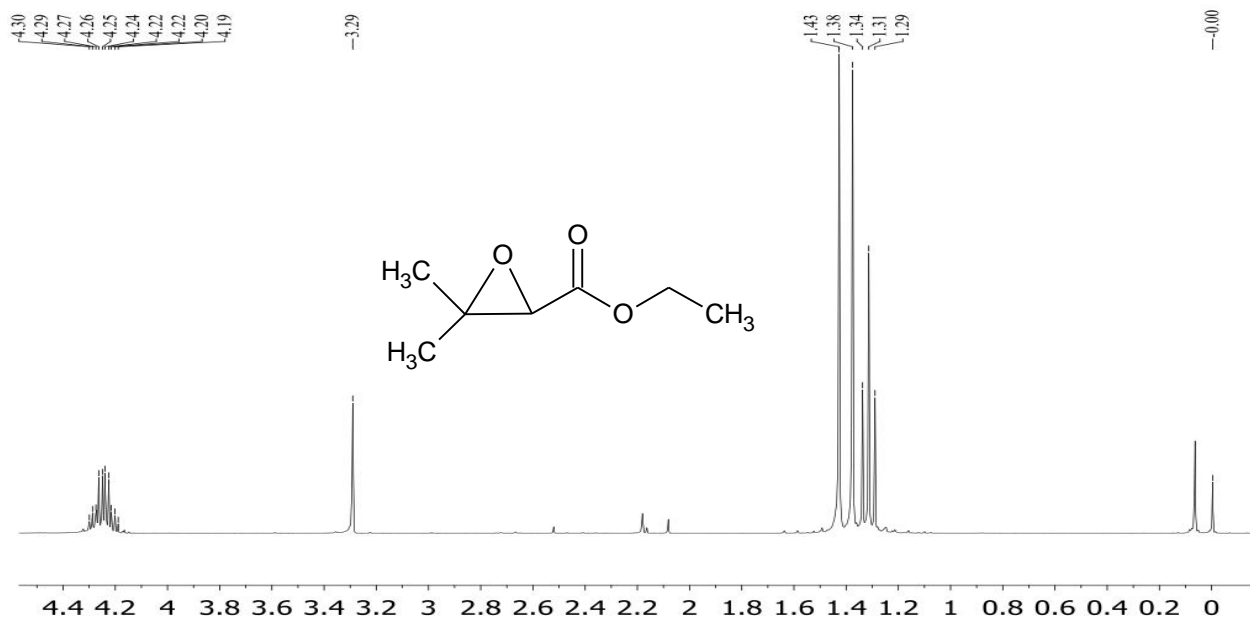
4. ^{1}H NMR of ethyl trans crotonate epoxide in CDCl$_3$.
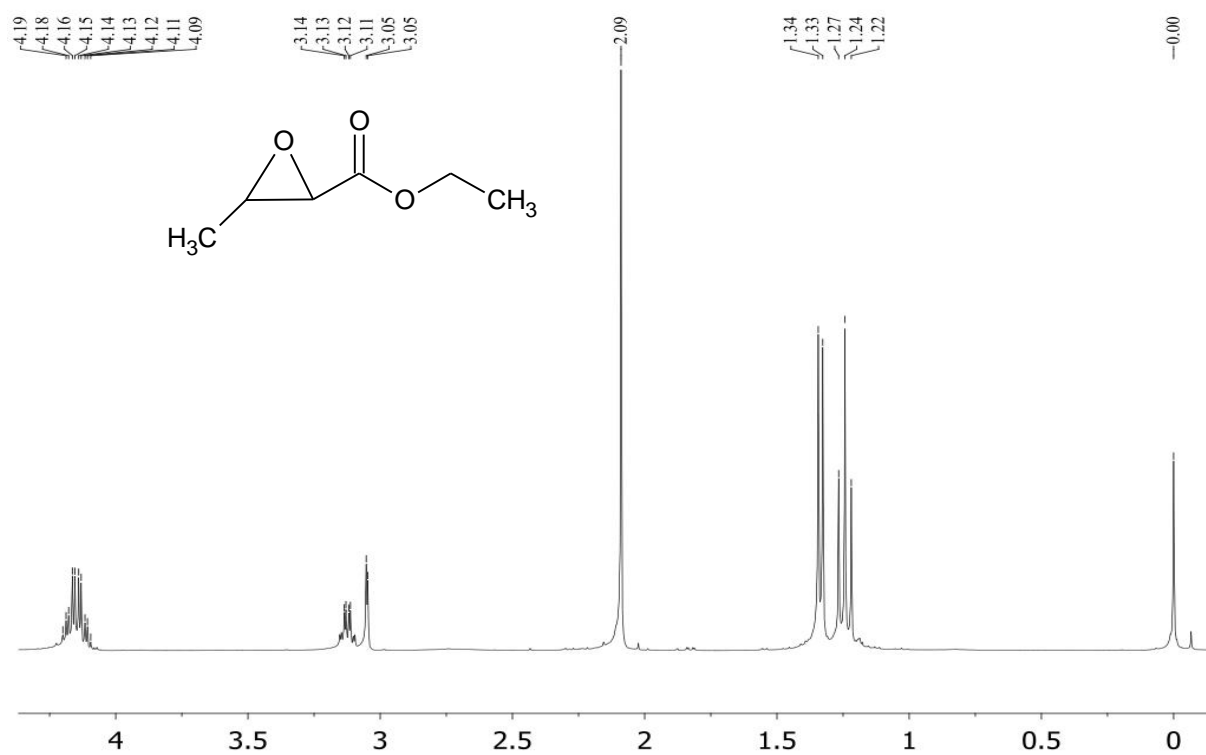
5. ^{1}H NMR of tert-butyl crotonate epoxide in CDCl$_3$.
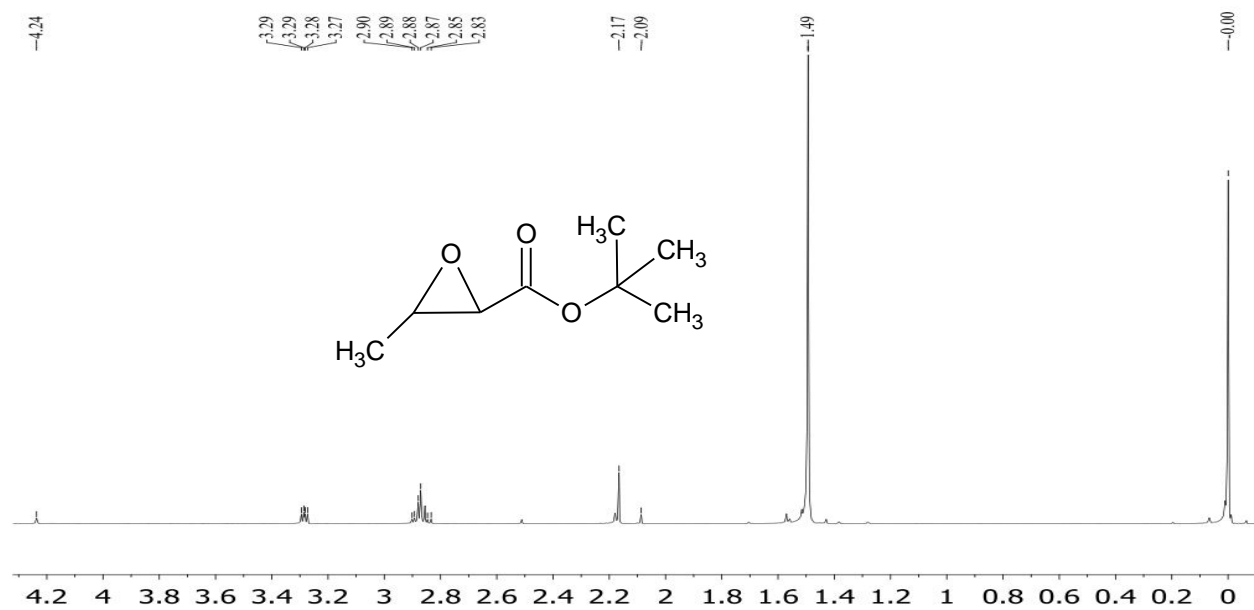
6. ^{1}H NMR of ethyl acrylate epoxide in CDCl$_3$.
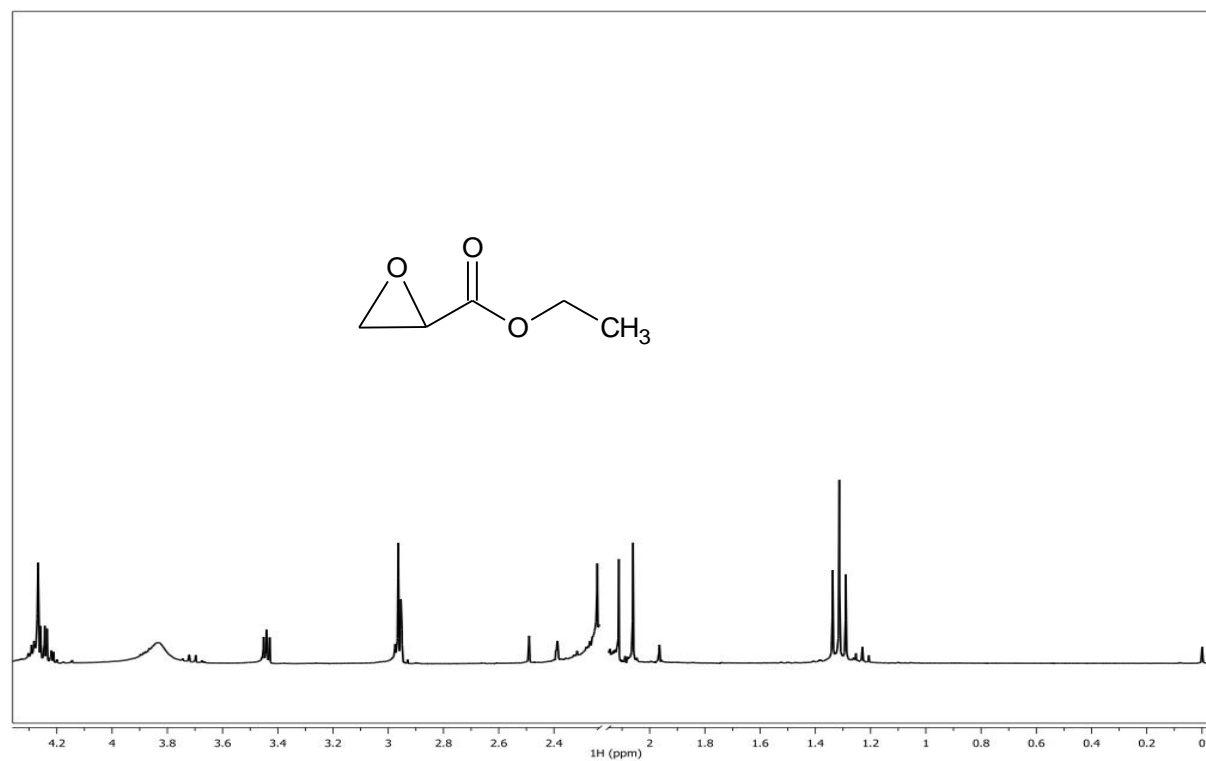
7. ^{1}H NMR of 1-methyl cyclopentene carboxylate epoxide in CDCl$_3$.
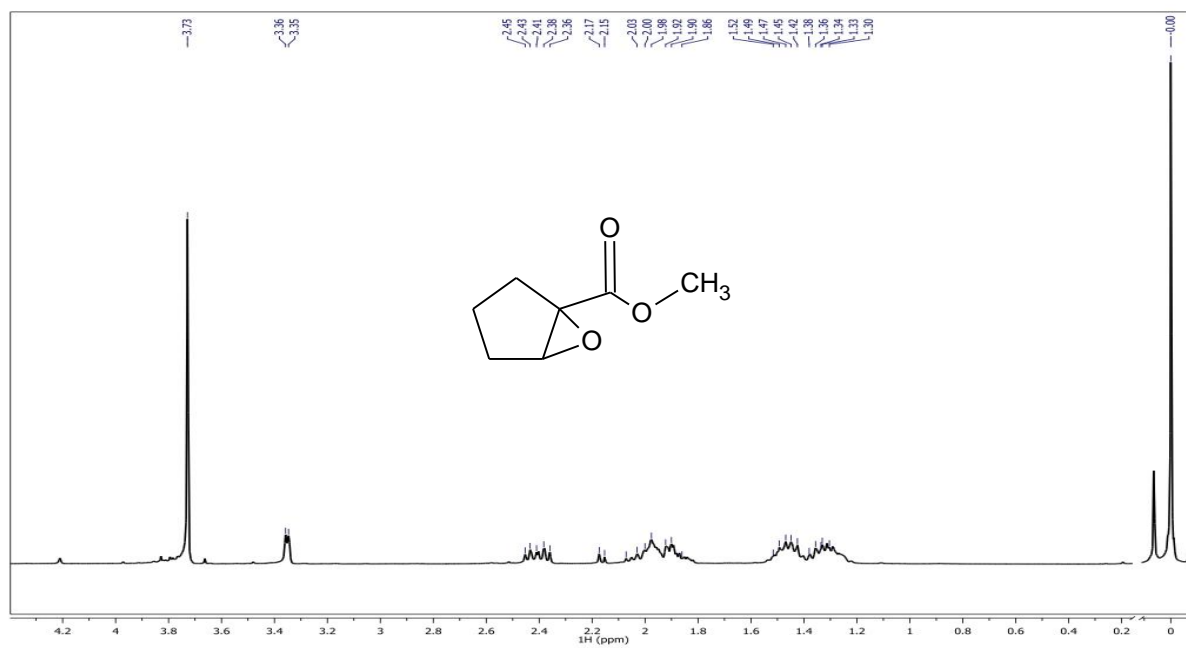
8. ^{1}H NMR of 1-methyl cyclohexene carboxylate epoxide in CDCl$_3$.
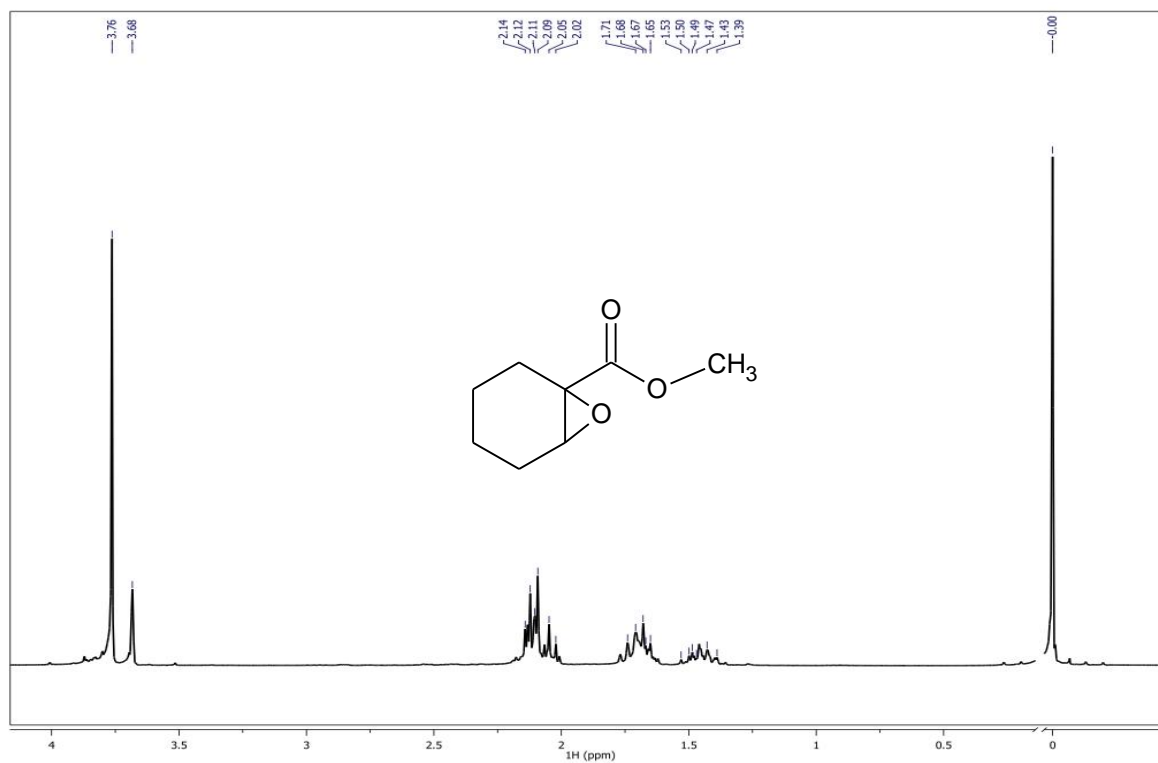
9. ^{13}C NMR of ethyl methacrylate epoxide in CDCl$_3$.
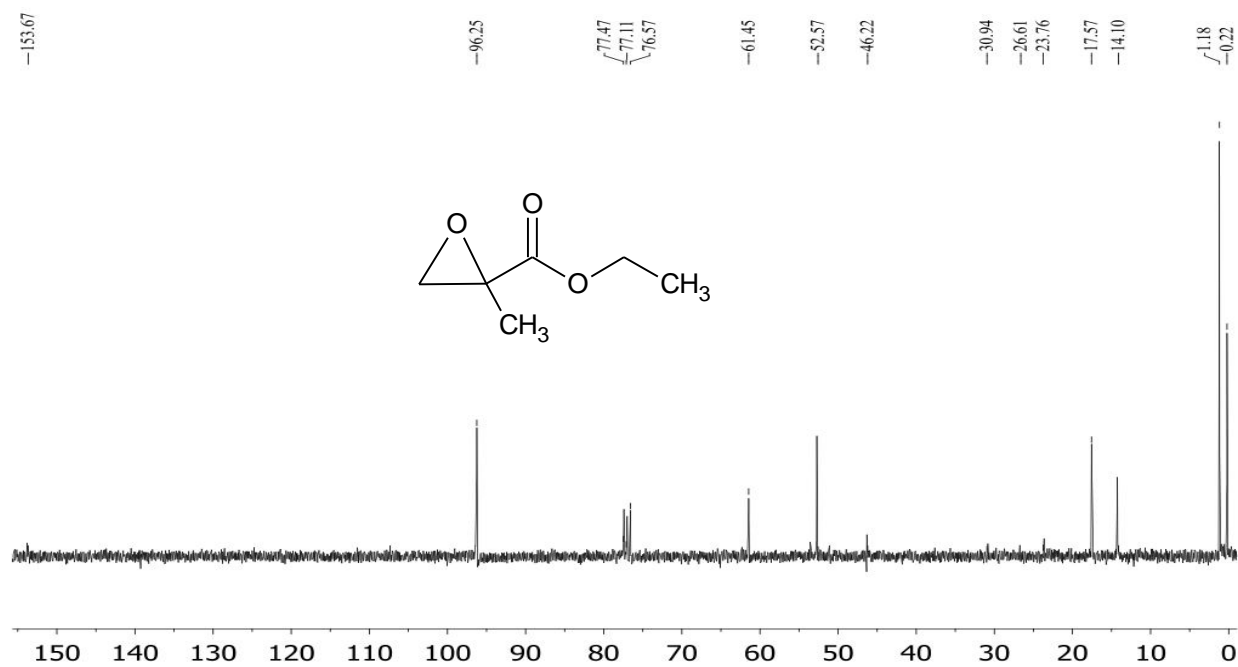

10. ^{13}C NMR of angelic methyl ester epoxide in CDCl$_3$.
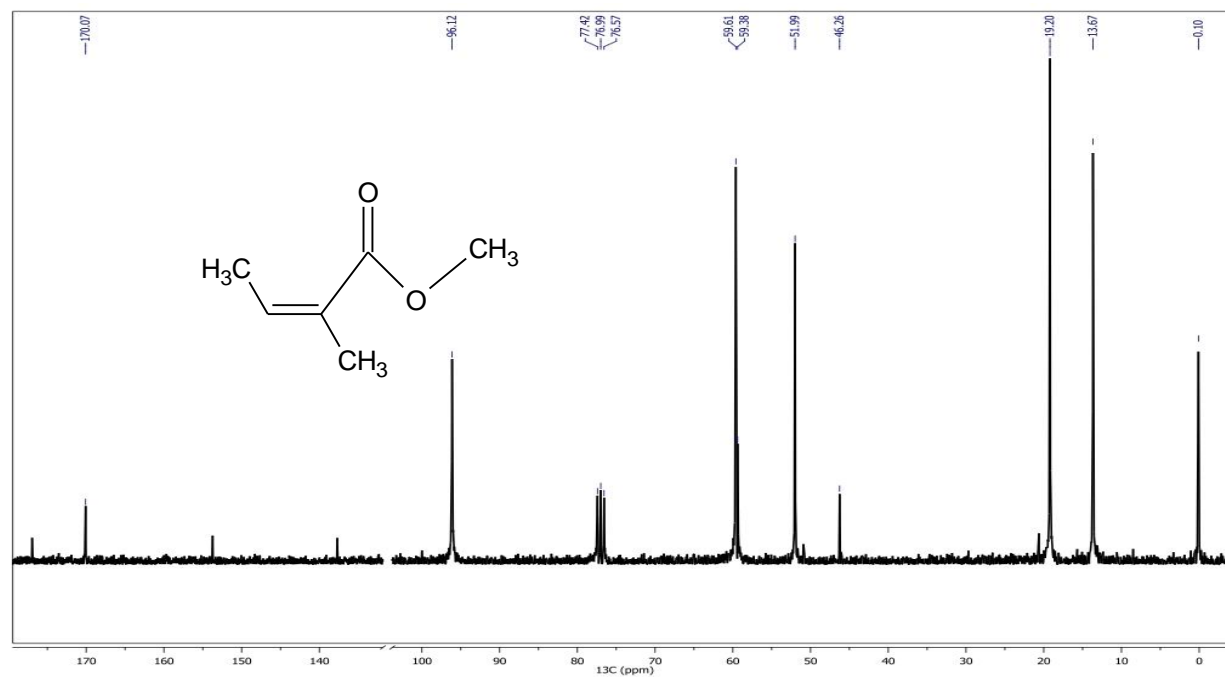
11. ^{13}C NMR of ethyl 3,3-dimethyl acrylate epoxide in CDCl$_3$.
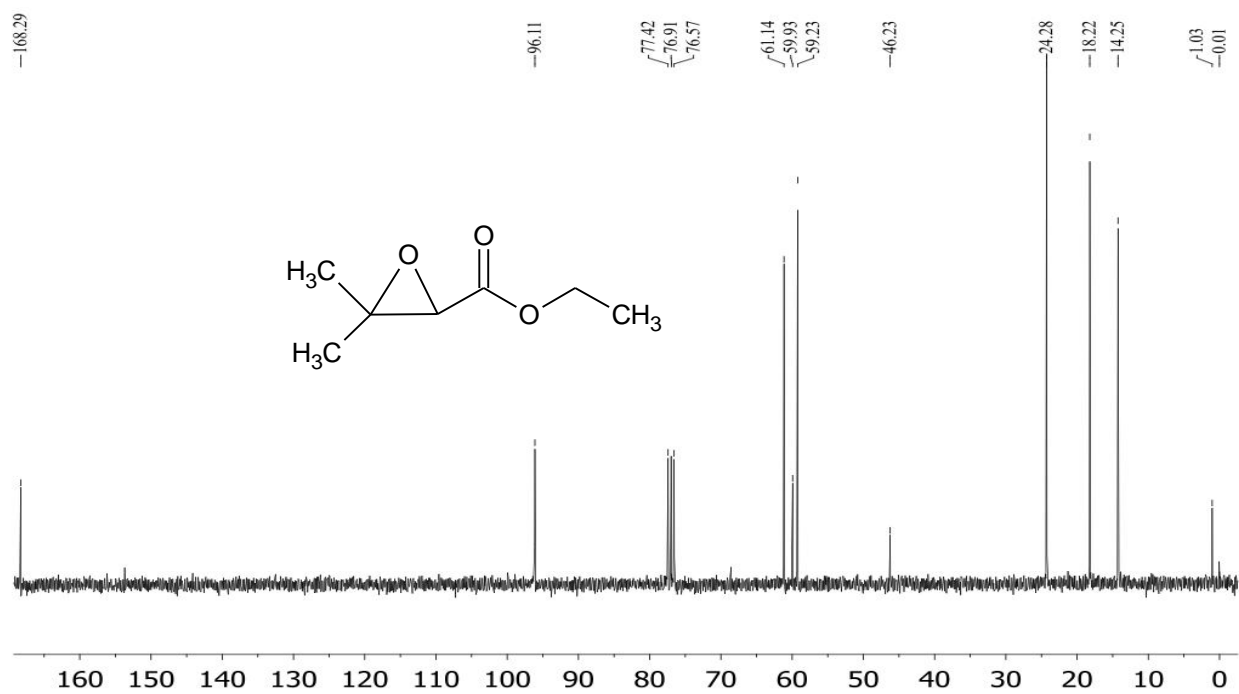
12. ^{13}C NMR of trans ethyl crotonate epoxide in CDCl$_3$.
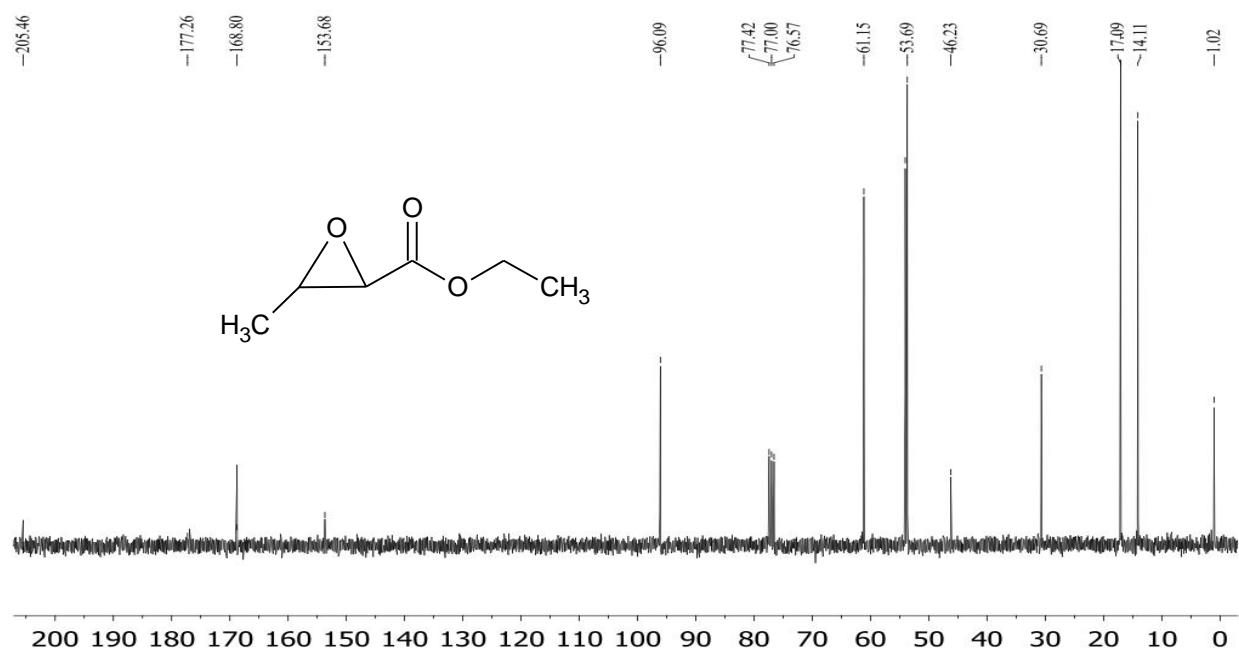
13. ^{13}C NMR of tert-butyl crotonate epoxide in CDCl$_3$.
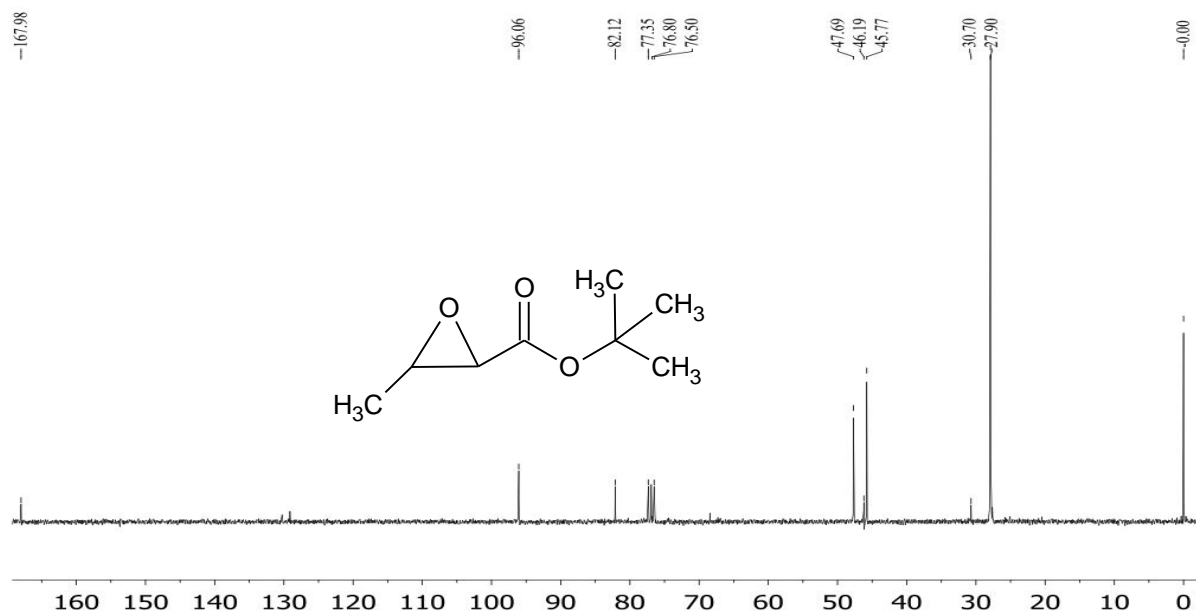

14. ^{13}C NMR of ethyl methacrylate epoxide in CDCl$_3$.
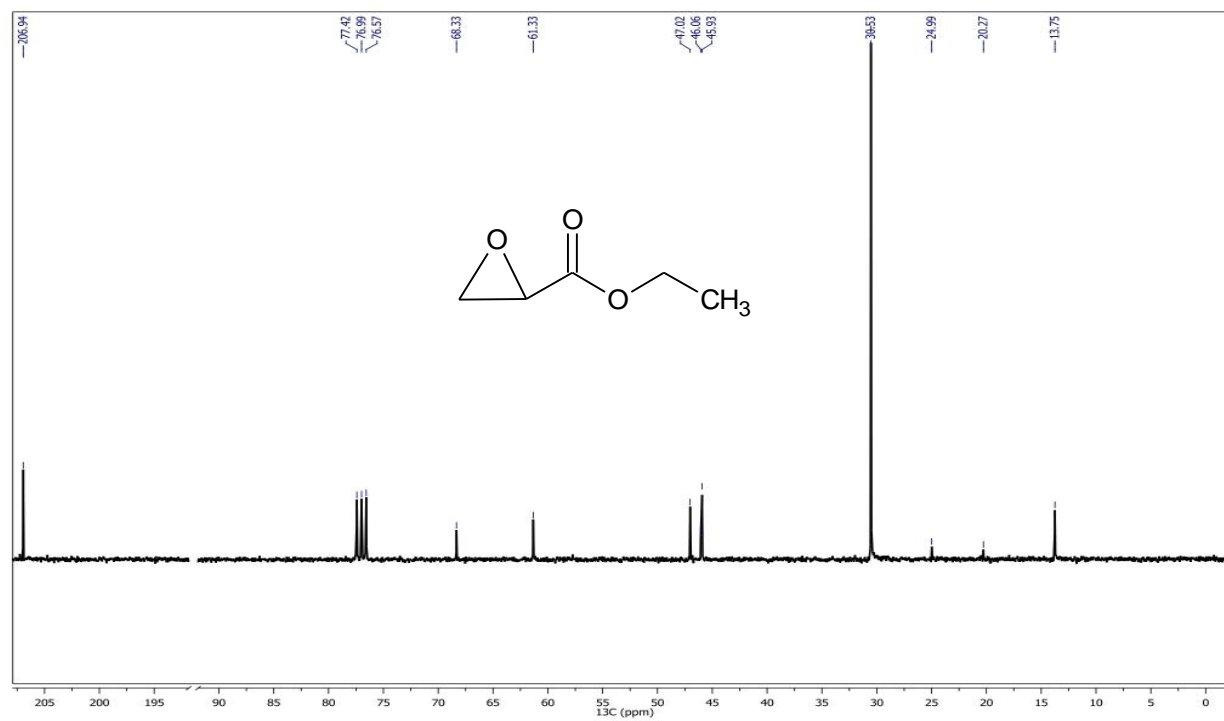
15. ^{13}C NMR of 1-methyl cyclohexene carboxylate epoxide in CDCl$_3$.
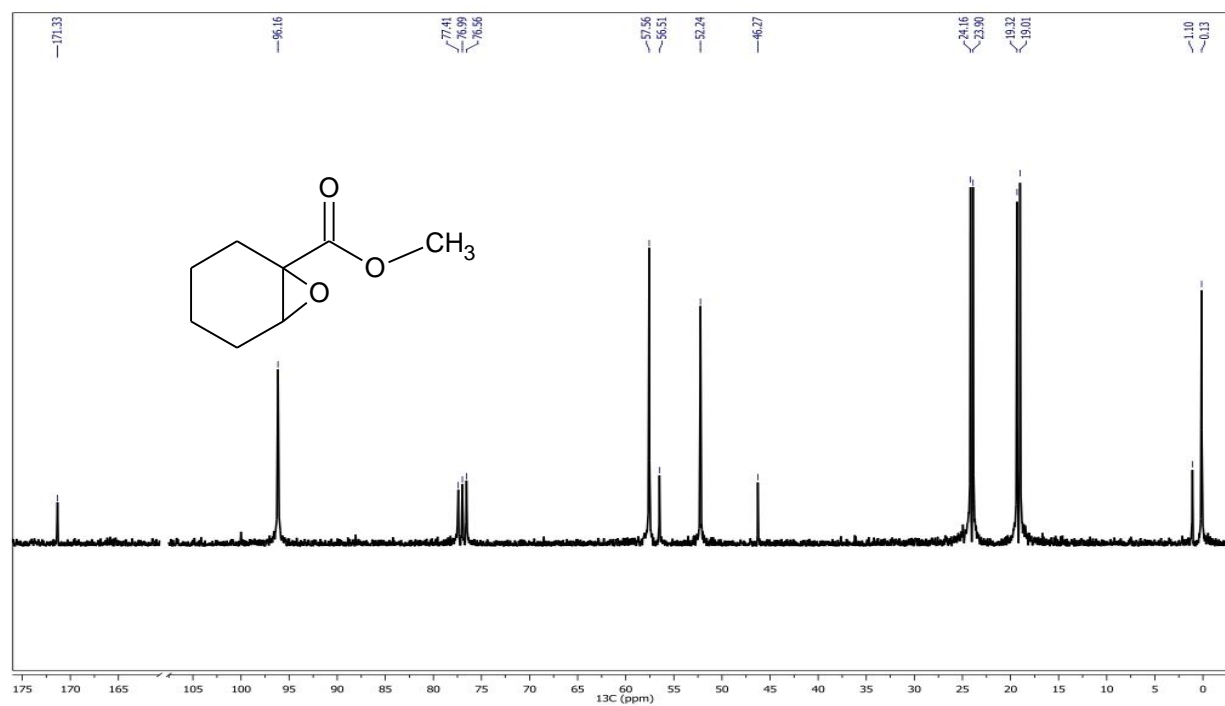
16. ^{13}C NMR of 1-methyl cyclopentene carboxylate epoxide in CDCl$_3$
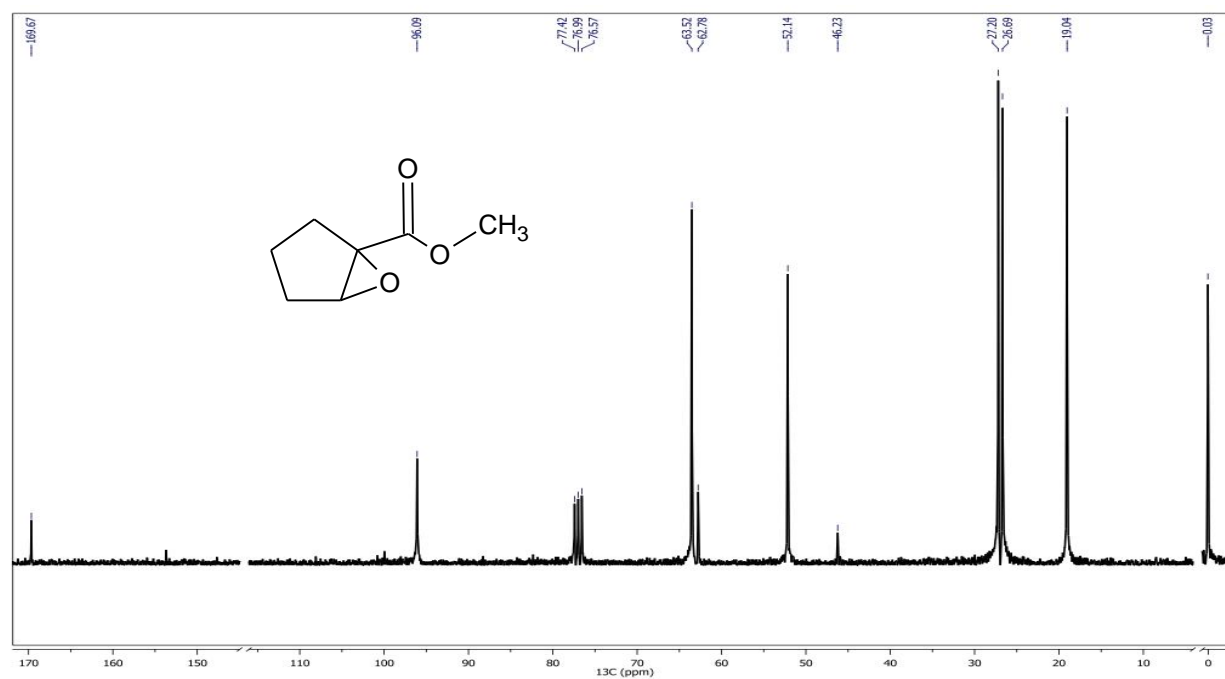
Appendix B: Comparison of kinetic data of angelic methyl ester with dimethyldioxirane at different molar ratios and concentrations
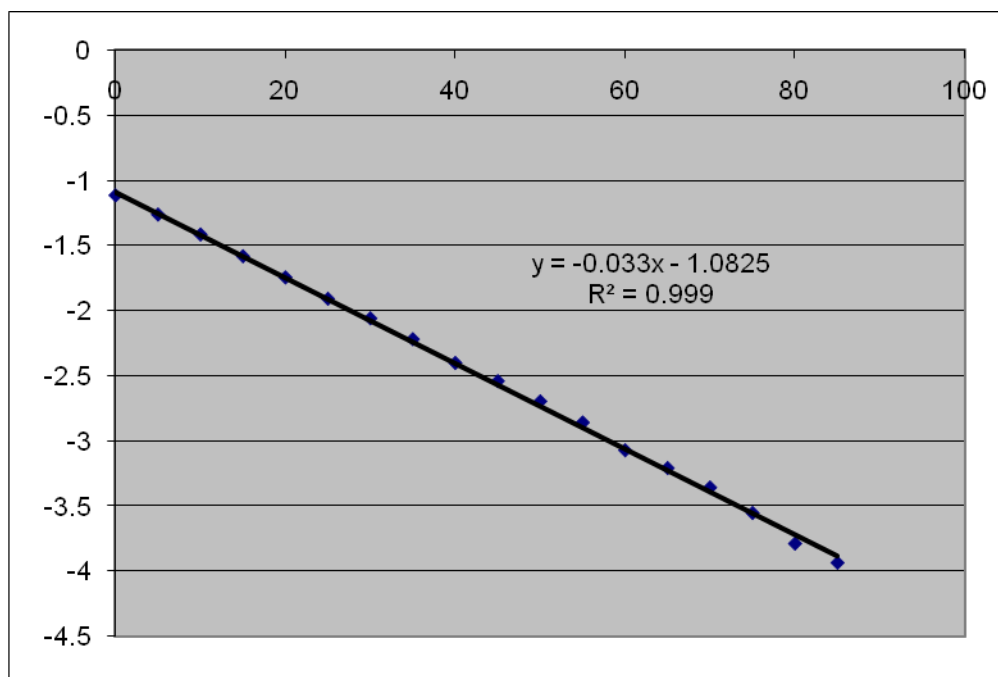
1. Natural log of absorbance of dimethyldioxirane with respect to time at 330 nm while undergoing reaction with angelic methyl ester in a 10:1 molar ratio.


$y = -0.0279x - 1.7068$
$R^2 = 0.9996$
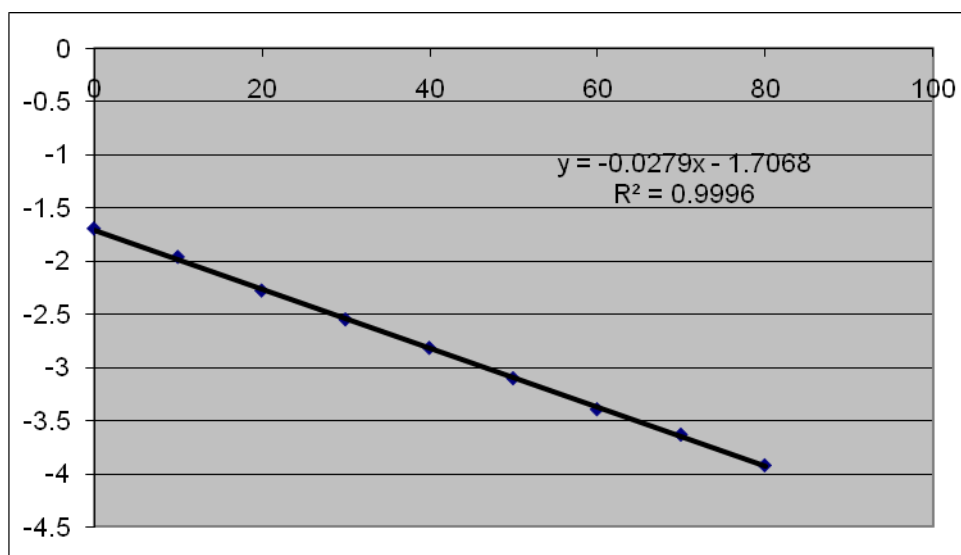
2: Natural log of absorbance of dimethyldioxirane with respect to time at 330 nm while undergoing reaction with ethyl tiglate in a 1:10 molar ratio.

$y = -3E-05x - 0.7196$
$R^2 = 0.7966$
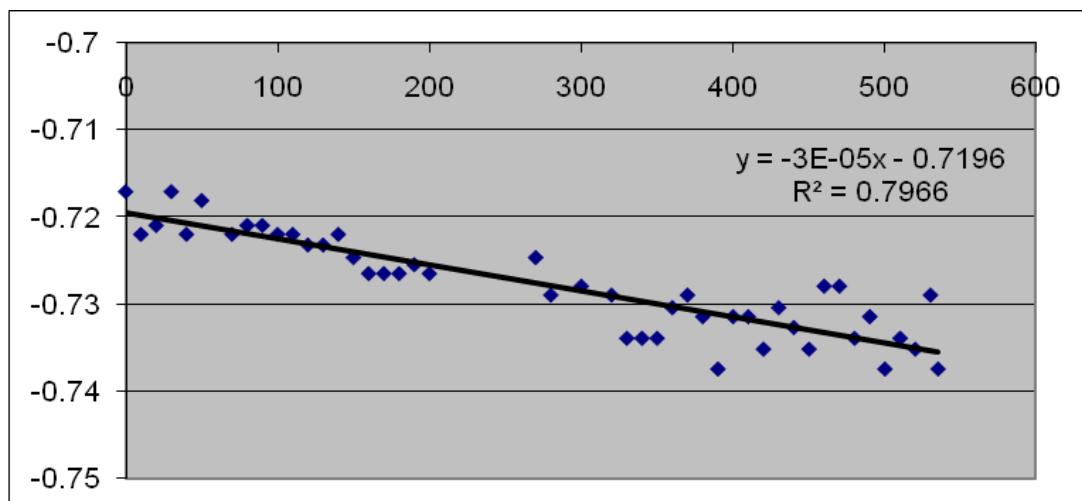
3: Natural log of absorbance of dimethyldioxirane with respect to time at 330 nm while undergoing reaction with angelic methyl ester with a higher concentration of reagents.

4: Natural log of absorbance of dimethyldioxirane with respect to time at 330 nm while undergoing reaction with angelic methyl ester with a lower concentration of reagents.
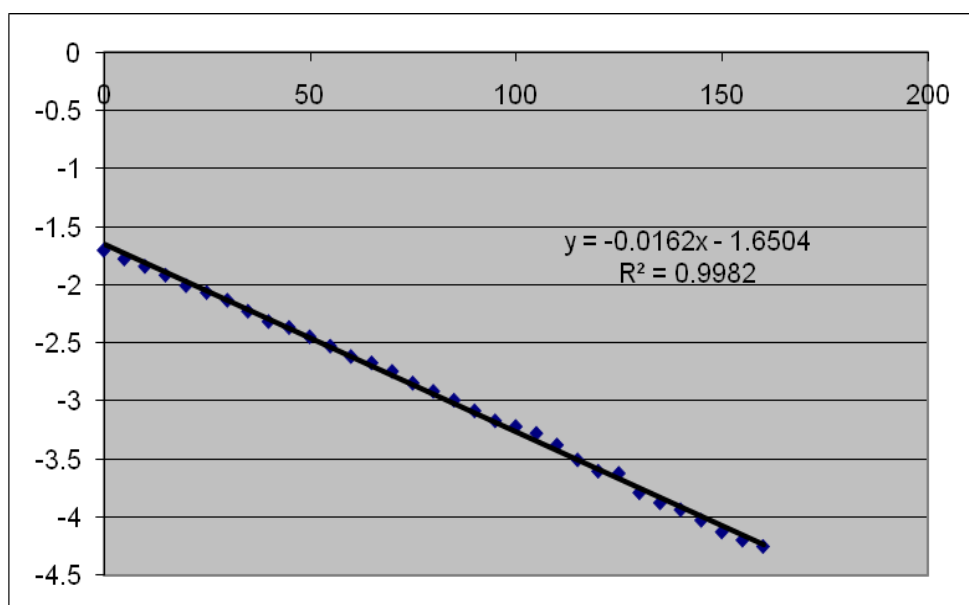
Appendix C: Computer data for $k_{2\ rel}$ of t-butyl crotonate

1. Computer calculation of $k_2$rel of tert-butyl crotonate

Ea calculation

	Ground State (Kcal/mol)	TS energy in (Kcal/mol)	TS energy out (Kcal/mol)	Ea in (Kcal/mol)	Ea out (Kcal/mol)
S-cis	-290894.293	-459168.759	-459166.241	28.529	31.047
S-trans	-290893.696	-459165.542	-459166.02	31.149	30.671

K_2rel calculation

Ester	Lowest Ea (Kcal/mol)	Weighted average Ea (Kcal/mol)	k_2 rel lowest energy	$k_2$rel weighted average
Methyl acrylate	28.53	29.45	1	1
t-butyl acrylate	29.31	29.11	3.73	1.78